

2013•2014  
FACULTEIT GENEESKUNDE EN LEVENSWETENSCHAPPEN  
*master in de biomedische wetenschappen: bio-elektronica  
en nanotechnologie*

## Masterproef

Optimization of a new SELEX process for the selection of novel  
17 $\beta$ -estradiol aptamers

Promotor :  
Prof. dr. Luc MICHIELS

Copromotor :  
dr. Veronique VERMEEREN

## Mehran Khorshid

*Masterproef voorgedragen tot het bekomen van de graad van master in de biomedische  
wetenschappen, afstudeerrichting bio-elektronica en nanotechnologie*

De transnationale Universiteit Limburg is een uniek samenwerkingsverband van twee universiteiten  
in twee landen: de Universiteit Hasselt en Maastricht University.



Universiteit Hasselt | Campus Hasselt | Martelarenlaan 42 | BE-3500 Hasselt  
Universiteit Hasselt | Campus Diepenbeek | Agoralaan Gebouw D | BE-3590 Diepenbeek



**Maastricht University**

2013•2014

FACULTEIT GENEESKUNDE EN  
LEVENSWETENSCHAPPEN

*master in de biomedische wetenschappen: bio-elektronica  
en nanotechnologie*

## Masterproef

Optimization of a new SELEX process for the selection  
of novel 17 $\beta$ -estradiol aptamers

Promotor :  
Prof. dr. Luc MICHIELS

Copromotor :  
dr. Veronique VERMEEREN

Mehran Khorshid

*Masterproef voorgedragen tot het bekomen van de graad van master in de biomedische  
wetenschappen, afstudeerrichting bio-elektronica en nanotechnologie*



## Acknowledgment

*“Two things awe me most, the starry sky above me and the moral law within me.”*

*Immanuel Kant*

All the work presented in this thesis was conducted at the Biomedical Research Institute (BIOMED) of Hasselt University, Campus Diepenbeek, Agoralaan Building C, BE 3590.

Foremost, I would like to express my sincere gratitude to my promoter, Prof. dr. Luc Michiels for giving me the opportunity to do my thesis in his group. All his support, immense knowledge and advice helped me throughout the period of my master thesis. Thanks a lot for the numerous things that I learned from him.

My special thanks goes to my co-promoter Dr. Veronique Vermeeren for her patience, motivation, as well as her precious remarks and guidance throughout the duration of this thesis. I deeply appreciate all her contributions towards the correction and completion of this thesis.

I am also indebted to my supervisor, Dra. Katrijn Vanschoenbeek for teaching me the scientific techniques required to carry out this thesis and for helping me out with lots of information regarding this master thesis. For sure, success in this thesis was impossible without her patience, motivation, as well as her friendly support.

My sincere appreciation goes to my dear professor and second examiner Prof. dr. Patrick Wagner, for all his kindness, friendly support and motivation. Thanks very much for many valuable things that I learned from him during this master course. It is my great pleasure to be his student.

I am highly grateful to thank Miss. Lotte Vanbrabant and Ms. Igna Rutten, for the laboratory assistance.

Also, my thanks go to my dear friend Drs. Kaushik Rajaram, Drs. Jeroen Vanbrabant and Dra. Natalie Vanden Bon for their kind assistance in the lab. I really enjoyed working in their group.

Thanks to my dear friends Theophilus Arebame and Heman Kumar Ramiya Ramesh Babu for their support. I will never forget the happy times that we had together.

Last but not the least, I would like to thank my dear family, especially my parents Abdolamir and Marzieh, for their faith in me and allowing me to be as ambitious as I wanted. For sure far away from them is very difficult for me.



## Table of contents

List of abbreviations .....	5
Abstract.....	7
1. Introduction.....	9
1.1 Endocrine Disruptive Chemicals (EDCs) .....	9
1.2 Biosensors .....	11
1.3 Surface Plasmon Resonance (SPR).....	12
1.4 Aptamer selection process .....	13
1.5 Biosensors for EDCs.....	14
1.6 Objective of research .....	15
2. Materials and Methods.....	17
2.1 Design of a ssDNA library.....	17
2.2 PCR optimization of the ssDNA library .....	17
2.3 SELEX .....	18
2.3.1 E2 and Nortestosterone Sepharose beads preparation .....	18
2.3.2 Counter selection step .....	19
2.3.3 Positive selection step .....	20
2.3.4 qRT-PCR and second melting curve analysis.....	20
2.3.5 Amplification of the bound aptamers and generation of ssDNA to be used in the next SELEX cycle.....	21
2.4 Sequence analysis .....	21
2.4.1 TOPO vector cloning, transformation, and colony PCR.....	22
2.4.2 EXO-SAP-IT purification and sequencing .....	22
2.4.3 Sequencing data analysis .....	23
2.5 Affinity and specificity studies of selected aptamers via SPR.....	23
2.5.1 SA-modified sensor chip immobilization .....	24
2.5.2 Affinity analysis of aptamers to E2.....	24
2.5.3 Specificity analysis of aptamers.....	24
2.5.4 SPR data analysis.....	25
3. Results and discussion .....	27
3.1 PCR optimization of the ssDNA library .....	27
3.2 SELEX process and ssDNA library enrichment .....	27
3.3 Colony PCR, sequencing and data analysis.....	31
3.4 Conformational analysis .....	34
3.5 Affinity and specificity studies of the selected aptamers.....	36

3.5.1 Affinity study of aptamers 1 and 2 for E2.....	38
3.5.2 Specificity study of different cholesterol derivatives.....	43
4. Conclusion .....	47
References.....	49

## List of abbreviations

- 2D: two-dimensional
- 3D: three-dimensional
- Aptasensors: Aptamer-based sensors
- ARs: Androgen Receptors
- bp: base pair
- BPA: bisphenol A
- BSA: Bovine Serum Albumin
- C<sub>T</sub>: threshold cycle
- CV: Cyclic Voltametry
- Da: Dalton
- DDT: dichlorodiphenyltrichloroethane
- DES: diethylstilbestrol
- dF1/dt: first derivative of the fluorescence response during the time
- DNA: Deoxyribonucleic acid
- dsDNA: double-stranded deoxyribonucleic acid
- *E. coli*: *Escherichia coli*
- E2: 17 $\beta$ -estradiol
- EDCs: Endocrine Disrupting Chemicals
- ERs: Estrogen Receptors
- FC: flow cell
- G: guanine
- GC/MS: Gas Chromatography/Mass Spectrometry
- Gel Doc: gel documentation
- HEPES: 4-(2-hydroxyethyl)-1-piperazineethanesulfonic acid
- hER: human Estrogen Receptor
- HPLC: High Performance Liquid Chromatography
- hr: hour
- IPCS: International Programme on Chemical Safety
- K<sub>a</sub>: association rate constant
- K<sub>A</sub>: equilibrium association constant
- K<sub>d</sub>: dissociation rate constant
- K<sub>D</sub>: equilibrium dissociation constant
- min: minute
- MW: molecular weight
- OH: hydroxyl group
- PBBs: polybrominated biphenyls
- PBS: Phosphate Buffered Saline
- PCBs: polychlorinated biphenyls
- PCR: Polymerase Chain Reaction
- PRs: Progesterone Receptors
- QCM: Quartz Crystal Microbalance
- QGRS: Quadruplex-forming G-Rich Sequences
- qRT-PCR: quantitative real-time PCR
- RI: Refractive Index
- RL: ligand response
- *R*<sub>max</sub>: maximum analyte binding response
- RNA: Ribonucleic acid
- rpm: Rotations per minute
- RRs: Retinoid Receptors

- RT: room temperature
- Rth: Heat Transfer Resistance
- RU: Response Units
- s: second
- SA: streptavidin
- SDS: sodium dodecyl sulfate
- SELEX: Systematic Evolution of Ligands by EXponential enrichment
- Sm: stoichiometry
- SOC: Super Optimal broth with Catabolite repression
- SPR: Surface Plasmon Resonance
- ssDNA: single-stranded deoxyribonucleic acid
- SWV: Square Wave Voltametry
- Ta: annealing temperature
- *Taq*: *Thermas aquaticus*
- TE: Tris/EDTA
- TIR: Total Internal Reflection
- TRs: Thyroid Receptors

## Abstract

Environmental and food-related residuals of natural and man-made EDCs are of concern due to their potential health hazards. It is believed that various health effects, including lowered fertility, endometriosis, and some cancers, are a result of exposure to EDCs. E2 and its analogues are one of the most important groups that interfere with the endocrine system. Therefore, to study them, detecting and measuring the concentration of these chemicals in complex samples is the most important challenge. Recently, Kim *et al.* (2007) introduced a prototype aptamer biosensor for E2 detection. These artificial oligonucleotides are being used as biological recognition elements, which their high stability and selectivity for small molecules, and their lower production cost compared with antibodies, making them advantageous.

The appealing features of aptamers prompted this thesis project, which was aimed to develop a new SELEX process for the selection of E2-aptamers in an optimized buffer composed of PBS and 10% ethanol, while Nortestosterone was used as counter molecule. It was hypothesized that such a SELEX can select aptamers with a high affinity and specificity to E2, especially for its hydroxylated aromatic ring A (phenolic group), according to the structural difference between E2 and Nortestosterone. Moreover, it was assumed that optimization of the buffer conditions for SELEX will allow, on the one hand, adequate dissolving of E2, and on the other hand, the selection of aptamers in experimentally realistic conditions. It was expected that selected aptamers in such realistic conditions will show lower unspecific binding and cross-reaction to molecules that are structurally similar to E2. Therefore, a more specific aptamer would be selected to fabricate a more efficient E2 aptasensor.

During the first step of this thesis, 12 iterative SELEX cycles were carried out on a pre-designed 80-mer ssDNA library, which was dissolved in the optimized buffer. After sequencing and structural analysis, the SELEX ended up with two aptamer molecules for E2. In the next step, both chemically synthesized biotinylated aptamers were immobilized on an SA-modified SPR sensor chip for affinity and specificity analysis. Under experimentally realistic conditions (e.g. PBS with 10% ethanol buffer, at RT) both selected sequences 2 and 1 showed good KDs (0.947 vs. 7.666  $\mu\text{M}$ , respectively), as well as a broad range of detection (0.36-11.47  $\mu\text{M}$  and 1.44-22.95  $\mu\text{M}$ , respectively) for E2. Specificity studies indicated a high selectivity of both sequence 2 and 1 for cholesterol derivatives with a phenolic group A epitope (17 $\alpha$ -ethinylestradiol, E2 and Estrone). In contrast to a previously selected 76-mer aptamer by Kim *et al.*, this epitope selectivity of the aptamers is due to a SELEX process targeting the structural difference between E2 and Nortestosterone.

In conclusion, this thesis project led to the selection of two ssDNA aptamers with high affinities and epitope selectivity to E2 molecule, which resulted to the fabrication of a novel SPR-based prototype E2 aptasensor. The advantageous epitope selectivity characteristic of our aptamers can give a highly reliable detection in complex samples, and it can push us some steps further to fabricate an array system for E2.



## 1. Introduction

The biosensor concept developed by Professor Clark in the middle of twentieth century, has opened a new era in monitoring and regulating a variety of parameters in areas such as hygiene, environmental protection, food industry, clinical diagnosis, drug development, or forensics. Biosensor technologists try to fabricate reliable analytical devices, with the simplest and cheapest of means, which are able to perform quick and accurate analyses in complex matrices. Application of these properly designed biosensors is the best solution to overcome many disadvantages of the complicated and expensive conventional methods [1].

During recent years, environmental and food-related residuals of Endocrine Disrupting Chemicals (EDCs) have become a concern due to their potential health hazards [2]. It is believed that various health effects, including lowered fertility, endometriosis, and some cancers, are a result of exposure to EDCs.  $17\beta$ -estradiol (E2) and its analogues are one of the most important groups that interfere with the endocrine system [3, 4]. Therefore, to study them, measuring the concentration of these chemicals in complex samples is necessary. High Performance Liquid Chromatography (HPLC), one of the routine monitoring methods in this field, has some limitations, such as a lack of real-time monitoring and its bulky size. Therefore, biosensors are good alternatives for on-site and real-time detection and measurement of EDCs, such as E2, in an easier, faster, and cheaper way. Aptamer-based sensors (aptasensors) are one type of biosensors, which have attracted particular attention for small molecule detection, especially E2, during the past years. In aptasensors, aptamers, which are oligonucleotides that take on a three-dimensional (3D) conformation, allowing them to recognize targets based on their topography, are being used as biological recognition elements, because of their high stability and selectivity for small molecules, and their low production cost [5].

In the following sections, EDCs and their relevant health hazards for humans and animals, as well as the biosensor concept, with special focus on aptasensors, will be reviewed. Furthermore, the idea and the objective of this research project will be discussed.

### 1.1 Endocrine Disruptive Chemicals (EDCs)

According to the 2002 International Programme on Chemical Safety (IPCS) document, an endocrine disruptor is described as “...an exogenous substance or mixture that alters function(s) of the endocrine system and consequently causes adverse health effects in an intact organism, or its progeny, or (sub) populations. A potential endocrine disruptor is an exogenous substance or mixture that possesses properties that might be expected to lead to endocrine disruption in an intact organism, or its progeny, or (sub) populations.” [6].

During the last decade, a variety of adverse effects of both natural and man-made EDCs on humans and animals have been observed [2]. Studies show that exposure to EDCs may result in health effects including breast and ovarian cancer, testes and prostate cancer, genital malformations, delayed sexual development, declining sperm count, obesity and neurological disorders such as delayed development of memory and intelligence [3, 4].

The mechanisms by which EDCs disrupt the actions of hormones have an enormous impact on the pattern of effects. Generally, EDCs can disrupt hormone action via two pathways. Firstly, they can have a direct competitive action on a hormone receptor protein complex including Estrogen Receptors (ERs), Androgen Receptors (ARs), Progesterone Receptors (PRs), Thyroid Receptors (TRs), and Retinoid Receptors (RRs), among others [3, 4]. Secondly, EDCs can have a direct action on a specific

protein, which controls the regulatory mechanisms of hormone delivery to the right place at the right time. These specific proteins could be involved in hormone production (e.g. aromatase), or they could be an important transporter (e.g. sodium/iodide symporter), or a carrier protein (e.g. cortisol binding protein). Therefore, EDCs can alter hormone synthesis, which leads to an increase or a decrease of the hormone levels in the blood. The impact of the altered hormone concentration would probably be similar to conditions where the hormone concentration in the body is changed because of disease or genetic disorders that inhibit or stimulate hormone synthesis. In contrast, the effects of an EDC can be quite complex if it interacts directly with a hormone receptor. Therefore, it should be expected to follow the mechanisms in which hormones interact with their receptors [4, 6].

The group of chemicals that are identified as EDCs is highly diverse. It consists of synthetic chemicals, such as industrial solvents or lubricants and their byproducts [polychlorinated biphenyls (PCBs), polybrominated biphenyls (PBBs), dioxins], plastics [bisphenol A (BPA)], plasticizers (phthalates), pesticides [methoxychlor, chlorpyrifos, dichlorodiphenyltrichloroethane (DDT)], fungicides (vinclozolin) and pharmaceutical agents [diethylstilbestrol (DES)]. Natural chemicals in food such as phytoestrogens, including genistein and coumestrol, also can act as EDCs [7].

E2 and its analogues are some of the most important EDCs that interfere with the endocrine system by binding to or blocking the ERs. These endocrine disruptors and their analogues in waste water or food products are of particular environmental concern [3]. E2 is one of the major sex hormones belonging to the steroid hormones. Based on a steroidal structure, E2 consists of four fused rings (A, B, C, and D) as well as two hydroxyl (OH) groups, which are attached to the aromatic ring A (making a phenolic group) and D (figure 1). E2 has a  $C_{18}H_{24}O_2$  formula with a molar mass of 272.38 g/mol [8]. E2 derivatives are the most important estrogen ingredients of combined oral contraceptive pills. E2 has been widely used as an anabolic steroid in animal fattening. Different studies clarify that EDCs, including E2, have harmful reproductive effects on aquatic wildlife. For instance, in fish these effects can be detected as sex reversals, production of intersex individuals, alterations in mating, and prevention of gonadal maturation. Moreover, humans are affected by chronic exposure to E2 and other EDCs, since these chemicals reach the natural aquatic systems and the drinking water [4, 9].

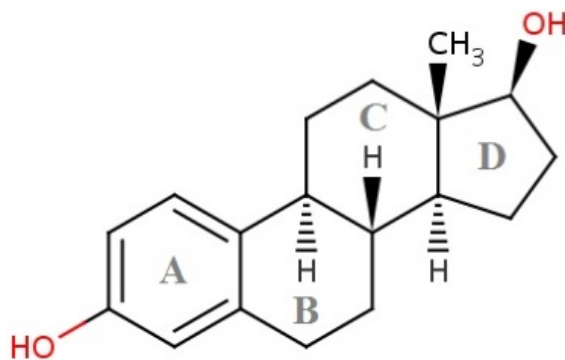


Figure 1:  $17\beta$ -estradiol (E2) structure. It consists of the fused rings A, B, C, and D, and two hydroxyl (OH) groups, which are attached to the aromatic rings A and D (shown in red).

## 1.2 Biosensors

Concerning the described health hazards of EDCs, e.g. E2, and the importance of their monitoring in food and environment, biosensors are good candidates for this purpose rather than other complicated conventional methods. Biosensors are compact analytical units that utilize biological recognition elements integrated with a physico-chemical transducer to determine the amount of a target biomaterial [10]. Target molecules can be captured by their specific biological recognition elements, including microorganisms, receptors, enzymes, antibodies and nucleic acids, which are attached to the transducer or sensor surface by means of covalent or non-covalent bonding. Binding of target molecules with the receptors leads to a physico-chemical alteration. This alteration is converted into a measurable output signal by the transducer. The intensity of the output signal is directly or inversely proportional to the concentration of the target molecule. Transducers can be subdivided into four main types: electrochemical, optical, piezoelectric and thermal transducers. Transducers send the generated output signal to the actuators, functioning as the biosensor reader unit. A graphical representation of a general biosensor is depicted in figure 2. Actuators with the related electronics or signal processors are primarily responsible for the display of the results [11, 12]. The ability to measure non-polar molecules that are not detectable by most other measurement devices, their increased specificity due to the immobilized recognition molecules, the possibility of rapid and continuous control, and their short response time, are the most important advantages of biosensors. However, the impossibility of heat sterilization due to the denaturation of the immobilized biological material, the danger of inactivating the biological material by exposure to extreme environmental conditions (e.g. pH, temperature, or ions), as well as fouling of the biosensor by other molecules that are capable of attaching non-specifically to the sensor surface are enumerated as their disadvantages. Good biosensors can be recognized based on their characteristics including high sensitivity, high specificity or selectivity, high precision, signal stability, fast working rate, fast response time, fast regeneration time, and reusability [13, 14].

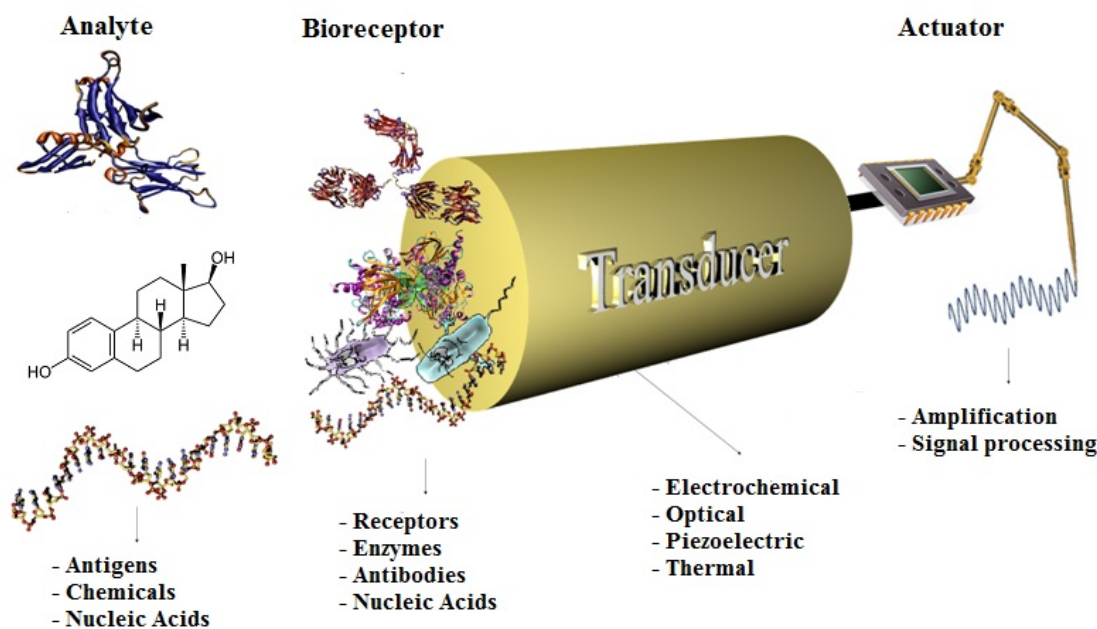


Figure 2: Principle of biosensors. A typical biosensor is composed of a bioreceptor layer attached to a transducer. The bioreceptors give the biosensor its specificity by selectively binding their target. The transducer is connected to an actuator which is responsible for amplification and signal processing.

A variety of biosensing principles, such as Surface Plasmon Resonance (SPR), Heat Transfer Resistance (Rth), Quartz Crystal Microbalance (QCM), and electrochemical biosensors, propose real-time and label-free methods for detection of the biomolecular interactions in samples.

In this research project SPR will be used as the detection principle, along with aptamers as the receptor molecules, to fabricate a novel E2 biosensor. Both the SPR and aptamers will be discussed in the next sections, separately.

### 1.3 Surface Plasmon Resonance (SPR)

SPR is known as an optical, yet label-free, detection process that happens when polarized light hits a prism with a high Refractive Index (RI) attached to a thin metal (gold) layer with a low RI. Usually, the incident light is reflected by the metal. However, under a certain wavelength, polarization, and incidence angle, called the resonance angle, none of the incident light is reflected, in a process called Total Internal Reflection (TIR), and free electrons at the surface of the metal layer will absorb incident light photons and convert them into surface plasmon waves. A dip in reflectivity of the light is seen under these conditions [15].

Interaction between immobilized probe molecules (ligands) and their target molecules (analytes) on the gold SPR chip surface induces variations in the RI of the gold chip surface due to a change in thickness of the biomolecular layer. The degree of change in the RI or thickness of the biomolecular layer can be significant since it represents the specific characteristics of the biomolecular interaction, e.g. the volume of biomolecules per unit area or the conformational folding of the molecules. As a result of RI alteration, the resonance angle of the incident light will change. The biomolecular interaction can be determined by examining the shift in resonance angle [16, 17]. This is shown in figure 3.

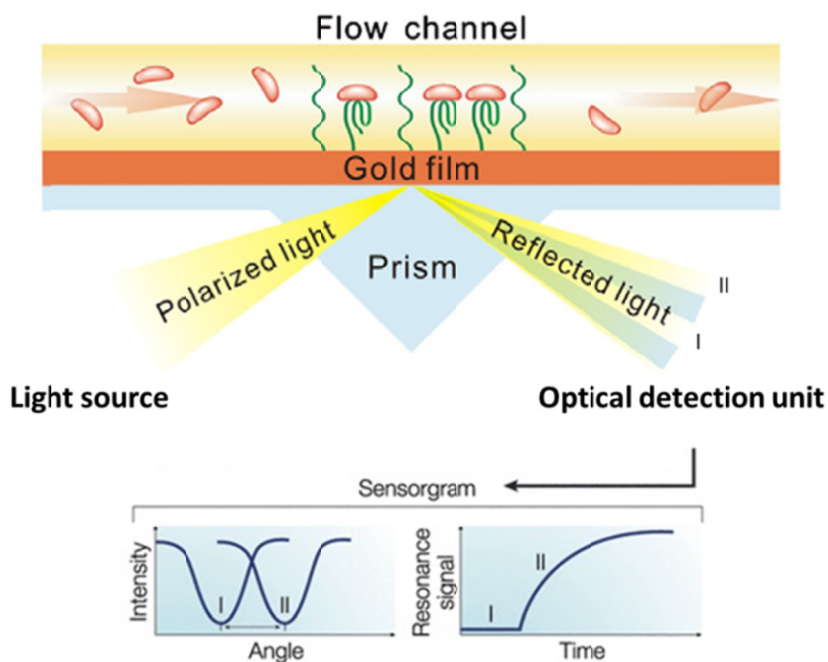


Figure 3: Principle of SPR. Ligands are immobilized on a gold layer, while the analyte molecules are flowed over the surface. Binding ligand to analyte will alter the surface RI. As a result of this alteration, the resonance angle of the incident light will change.

## 1.4 Aptamer selection process

Aptamers refer to a class of molecules including oligonucleotide or peptide sequences which are able to identify virtually any class of target molecules with high affinity and specificity. Their binding ability is due to structural compatibility, stacking of aromatic rings, electrostatic forces, hydrogen bonding or a combination of all these effects. Their advantages, such as their specific binding ability to the target molecules, low production cost, as well as higher stability in comparison with antibodies as their natural rivals, make them good candidates for therapeutic and diagnostic purposes. Aptamers are usually generated by a selection process from a large random pool (library) of sequences, but they also exist naturally as riboswitches [18, 19, 20].

Aptamers are created by Systematic Evolution of Ligands by EXponential enrichment (SELEX), an *in vitro* selection process. In this method, unique RNA or DNA molecules with a very high affinity and specificity for target molecules are selected by exposing a very large library of random sequence oligomers (DNA or RNA library) to this target. The complexity of the library is dependent on the number of randomized nucleotides. Normally, the starting SELEX round contains around  $10^{15}$  individual sequences, a very large number that permits a high probability of selecting a specific aptamer for the target of interest [18].

Typically, for DNA aptamer selection, chemically synthesized random linear nucleotide sequences, which are flanked by two known primer binding sequences, are mixed with the target molecule immobilized on a matrix (e.g. Sepharose or magnetic beads, columns, polystyrene plates, etc.) via functional groups and allowed to form complexed structures. Following this, weakly and non-bound single stranded DNA (ssDNA) sequences are separated from tightly bound ones. The tightly bound sequences are eluted by a denaturing process. These eluted sequences are amplified by Polymerase Chain Reaction (PCR) and in the next step the amplified sequences, in the form of double stranded DNA (dsDNA), are converted to ssDNA via enzymatic digestion or linear amplification before starting a new SELEX cycle. The procedure of SELEX is graphically displayed in figure 4. All the steps are repeated until the sequences that bind tightly to the target are enriched. The number of required cycles is dependent on the stringency imposed on each round, as well as on the affinity of interaction between the target and the aptamers. In general, around 8–15 cycles are needed before selecting an oligonucleotide population that is dominated by those sequences which bind the target best. Potentially, each cycle can be composed of positive, negative, and counter selection steps depending on the SELEX process and the target molecule. Both negative and counter selection steps minimize the co-selection of unwanted aptamers. Aptamers that bind to the immobilization matrix as well as aptamers that are unable to discriminate between closely related structures are deleted from the library during negative and counter selection steps, respectively. It should be noted that the steps for positive, negative, and counter selection are similar, except that the counter molecules for the counter selection are analogue molecules to the target with some structural differences to increase the selectivity of the obtained sequences, while the immobilization matrix with no attached target molecule is used during negative selection. Also, unlike in the positive step, in the negative or counter selection step the unbound sequences will be used for future cycles. The negative selection step can be discarded using blocking agents [e.g. Bovine Serum Albumin (BSA)] to cover free spaces over the immobilization matrix during positive and counter selection steps [18, 20]. Cycle after cycle, the amount of DNA sequences that bind to the target with high affinity will become more numerous in the library, i.e. they will become enriched. After molecular enrichment in the pool, cloning and sequencing of the selected aptamers will allow them to be generated by chemical synthesis.

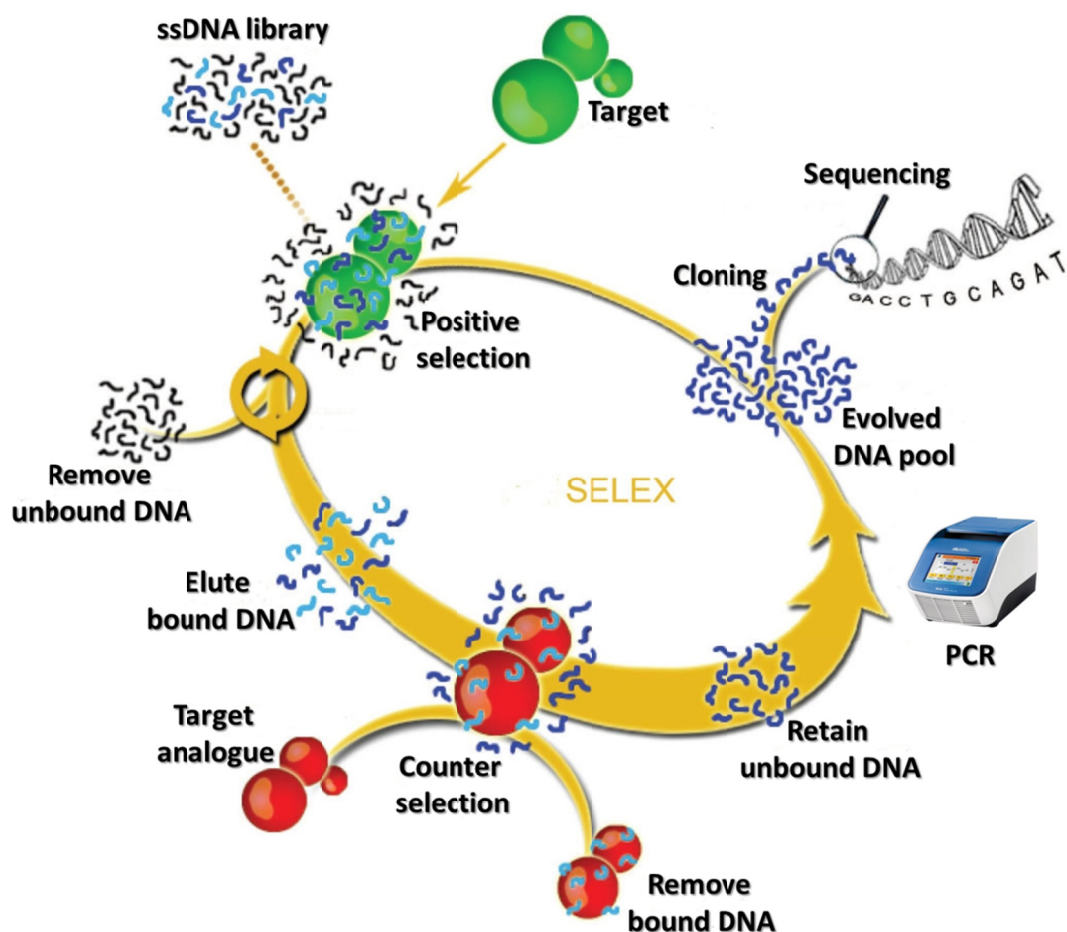


Figure 4: A typical SELEX procedure. Each SELEX cycle consists of counter and positive selection steps, without negative selection step. The bound DNA to the counter molecule will be deleted from the SELEX, while the bound ones to the target molecule will be eluted to continue the process.

### 1.5 Biosensors for EDCs

Up till now, different analysis methods, such as HPLC or Gas Chromatography/Mass Spectrometry (GC/MS), have been used as highly sensitive techniques to detect EDCs in complex environmental samples. However, these methods have some limitations, like the lack of real-time monitoring applications or complicated procedures. Therefore, developing a simpler and more accurate biosensor has been the focus of much research [5]. Commonly, in biosensor systems for E2 detection, the human Estrogen Receptor (hER) has been used. These biosensors can detect estrogenic chemicals, including E2, with high sensitivity, but with low specificity because of the affinity of the receptor for other xenoendocrines [21]. Cell-based biosensors represented another generation. They were constructed with recombinant cells harboring the hER promoter and lacZ as the reporter gene. These assays can give good information about the concentration level of EDCs, including E2, and about their action inside the cell, but their application is limited due to a long detection time, as well as low specificity due to the affinity of hER to a wide range of EDCs [22]. Recently, more sensitive and rapid methods, such as immunoassays and biosensors using nanoparticles, have been developed for the detection of E2. The specificities of these biosensors were reported to be better than hER-based biosensors due to their structure-specific biorecognition [23, 24].

In 2007, Kim *et al.* introduced a prototype aptasensor for E2 detection. In this type of biosensor, aptamers are being used as biological recognition elements, with their high stability and selectivity for small molecules, and their lower production cost compared with antibodies, making them advantageous [5]. Moreover, the interaction between aptamers and their target can be broken, unlike that between antibodies and antigens, giving the resulting aptasensor a reusable character. These appealing features prompted this thesis project, aiming to generate aptamers to detect E2, that can eventually be implemented as bioreceptors in an aptasensor.

## 1.6 Objective of research

Recent efforts by the Nanobiotechnology research group at Hasselt University have resulted in the selection of two DNA aptamer batches for E2. Each aptamer batch was selected based on 8 SELEX cycles in 4-(2-hydroxyethyl)-1-piperazineethanesulfonic acid (HEPES) buffer, and the analogues Dexamethasone and Nortestosterone were used as the binding molecules during the counter selection steps for each SELEX. Affinity studies of the two aptamer batches showed sensitivity and specificity to the target molecule and to some of its analogues. The cross-reactivity of the aptamers to the target and its analogues is assumed to be due to the structural similarity between the analogues and E2. However, using HEPES buffer as a working solution during affinity studies with SPR can be a confounding variable on the SPR signal due to its high molecular weight and subsequent effect on the surface of the sensor. Furthermore, ethanol is necessary to dissolve E2 during binding studies with SPR. Because of the fact that ethanol was not present in the SELEX buffer during aptamer selection, and that the secondary structure of aptamers, as well as their binding ability, is dependent on the buffer composition, it is suspected that ethanol can affect the binding efficiency of the selected aptamers to their target.

Concerning all the described problems and criteria, the aim of this project is to select new aptamers for E2 in an optimized buffer composed of ethanol and Phosphate Buffered Saline (PBS). Moreover, Nortestosterone is going to be used during the counter selection step. Such a SELEX process can result in aptamers with a high affinity for E2, especially for the hydroxylated aromatic ring A (phenolic group), based on the structural difference between E2 and Nortestosterone. Moreover, it is assumed that optimization of the buffer conditions for SELEX will improve the binding studies of the aptamer to the target molecule. The methodology of the project will be based on the developed procedures at the Nanobiotechnology laboratory of the Hasselt University. The research will be composed of four main domains, including the design and testing of the ssDNA library, optimizing the SELEX procedure composed of counter (Nortestosterone) and positive (E2) selection steps in the new PBS and ethanol buffer, sequence analysis, and affinity and specificity studies of the selected aptamers via SPR binding assays.



## 2. Materials and Methods

### 2.1 Design of a ssDNA library

The ssDNA library consisted of a 40 base random region flanked by two fixed primer binding regions of 20 bases each (5'-TGT GTG TGA GAC TTC GTT CC-40 random nucleotides-CAG CAA GGC ATC AGA GGT AT-3'). The library and associated primers were designed and evaluated by using Oligo<sup>®</sup> software (version 7.56), according to the criteria shown in table 1, and obtained from Integrated DNA Technologies, Inc. (IDT, Leuven, Belgium).

Table 1: Primer design evaluation criteria and primer specifications

Criteria	Forward Primer specification	Reverse Primer specification
Sequence	5'-TGT GTG TGA GAC TTC GTT CC-3'	5'-ATA CCT CTG ATG CCT TGC TG-3'
Length (18-22 nucleotides)	20 nucleotides	20 nucleotides
G+C content (50-55%)	50%	50%
Melting temperature ( $T_m=50-60^\circ\text{C}$ )	56.8 $^\circ\text{C}$	56.7 $^\circ\text{C}$
Maximum accepted stability of hairpins ( $\Delta G > -3$ kcal/mol)	0 kcal/mol	0 kcal/mol
Maximum accepted stability of self or cross dimers ( $\Delta G > -6$ kcal/mol)	-0.8 kcal/mol	-1.5 kcal/mol
Maximum accepted stability of heterodimers ( $\Delta G > -6$ kcal/mol)	-1.3 kcal/mol	

### 2.2 PCR optimization of the ssDNA library

The optimal annealing temperature ( $T_a$ ) of the primers was determined by performing a gradient PCR. All the reactions were carried out in a Veriti<sup>™</sup> Thermal Cycler (Applied Biosystems, Darmstadt, Germany). The 50  $\mu\text{l}$  PCR reaction mix was made up of 5  $\mu\text{l}$  10 $\times$  PCR buffer (Roche, Vilvoorde, Belgium), 2.5  $\mu\text{l}$  of 50 mM  $\text{Mg}^{2+}$  (Roche) (totalling 4 mM  $\text{Mg}^{2+}$  in the reaction, including the  $\text{Mg}^{2+}$  present in 10 $\times$  PCR buffer), 1  $\mu\text{l}$  of 0.01 mM forward primer, 1  $\mu\text{l}$  of 0.01 mM reverse primer, 2.5  $\mu\text{l}$  of 20 mM dNTPs (Roche), 1  $\mu\text{l}$  of 5 U/ $\mu\text{l}$  *Taq* DNA polymerase (Roche), 1.7  $\mu\text{l}$  of 0.0001 mM ssDNA library, which contains  $10^{11}$  molecules, and deionized water up to 50  $\mu\text{l}$ . The reaction mix was thermally cycled as shown in table 2.

For a better yield of PCR products, different concentrations of  $\text{Mg}^{2+}$  as well as different amounts of ssDNA library were tested. The thermal conditions and reaction mixture were the same as described before, except a 2.5  $\mu\text{l}$  and 1.2  $\mu\text{l}$  of 50 mM  $\text{Mg}^{2+}$  was evaluated with an input of 17  $\mu\text{l}$ , 1.7  $\mu\text{l}$ , and 0.17  $\mu\text{l}$  0.0001 mM ssDNA library.

Table 2: Gradient PCR program

Process	Number of cycles	Temperature ( $^\circ\text{C}$ )	Time
Initial denaturation	1	95	10 min
Amplification	30	95	30 s
		<sup>1</sup> $T_a$	30 s
		72	30 s
Final extension	1	72	10 min
Cool-down	1	4	$\infty$

<sup>1</sup> $T_a$  was a spectrum from 48 to 60 $^\circ\text{C}$ , with 2 $^\circ\text{C}$  increments.

All the PCR products were analyzed on a 4% agarose gel (Invitrogen, Ghent, Belgium) and the length was compared with a 25 and 100 base pair (bp) DNA ladder (Invitrogen) on a Bio-rad gel documentation (Gel Doc) system (Bio-rad Laboratories Inc., Brussels, Belgium).

## 2.3 SELEX

The SELEX process was composed of 12 repeated cycles including positive and counter selection steps. E2 and Nortestosterone, attached to Sepharose beads (Polysciences Inc., Warrington, USA), were used as target and counter molecule, respectively. The first SELEX cycle was composed of four counter, one positive and one counter selection step. The order from the second SELEX cycle on was one counter, one positive and one counter selection step. During each cycle, quantitative real-time PCR (qRT-PCR) and second melting curve analysis were used for the determination of the molecule number, and the enrichment of the selected aptamer molecules in all the positive and counter selection steps, respectively. After the last counter selection step at the end of each cycle, the ssDNA library was conditioned for the next SELEX cycle. This final process step was composed of a PCR amplification with native forward and phosphorylated reverse primers, a subsequent purification of the target sequences on 4% agarose gel, and generating ssDNA from the dsDNA PCR products via Lambda exonuclease digestion. The optimized procedure is graphically displayed in figure 5.

### 2.3.1 E2 and Nortestosterone Sepharose beads preparation

Concerning the number of positive and counter selection steps per cycle, about 150  $\mu$ l E2 and 150  $\mu$ l Nortestosterone Sepharose beads were each divided into three fractions. After a mild vortex and centrifugation (Eppendorf, Hamburg, Germany) step at 3200 rotations per minute (rpm) for 2 minutes (min), the supernatant was discarded. A single washing step with 1 $\times$  PBS pH 7.4 (1.29 M NaCl, 15 mM  $\text{KH}_2\text{PO}_4$ , and 61.4 mM  $\text{Na}_2\text{HPO}_4$ ) for 5 min on a rotor (Dyna<sup>®</sup> sample mixer, Life Technologies, Ghent, Belgium) was followed by a new centrifugation and supernatant withdrawal. A blocking step was done by incubating one fraction of both types of beads with 0.015 g BSA (United States Biological, Swampscott, USA) in 1 ml 1 $\times$  PBS, a second fraction of each with 0.015 g dried skimmed milk or Marvel (Premier International Foods, Dublin, Ireland) in 1 ml 1 $\times$  PBS, and the third fraction with 40  $\mu$ l synthetic blocking reagent NB3025 (Cosmo Bio Co., Tokyo, Japan) in 960  $\mu$ l 1 $\times$  PBS for at least 2 hours (hr) at room temperature (RT) on a rotor. Subsequently, 3 washing steps with 1 $\times$  PBS followed while combining all the blocked fractions of E2 and Nortestosterone beads together. Ultimately, the beads were blocked with 5 mg/ml non-specific sonicated salmon sperm DNA (Invitrogen) in 1 ml 1 $\times$  PBS on a rotor overnight at 4 $^\circ$ C. Three washing steps were performed, first with 1 $\times$  PBS containing 0.5% tween 20 (PROLABO<sup>®</sup>, Paris, France), and subsequently twice with 1 $\times$  PBS. Finally, after adding 500  $\mu$ l of 1 $\times$  PBS the beads were kept at 4 $^\circ$ C until usage in the selection steps.

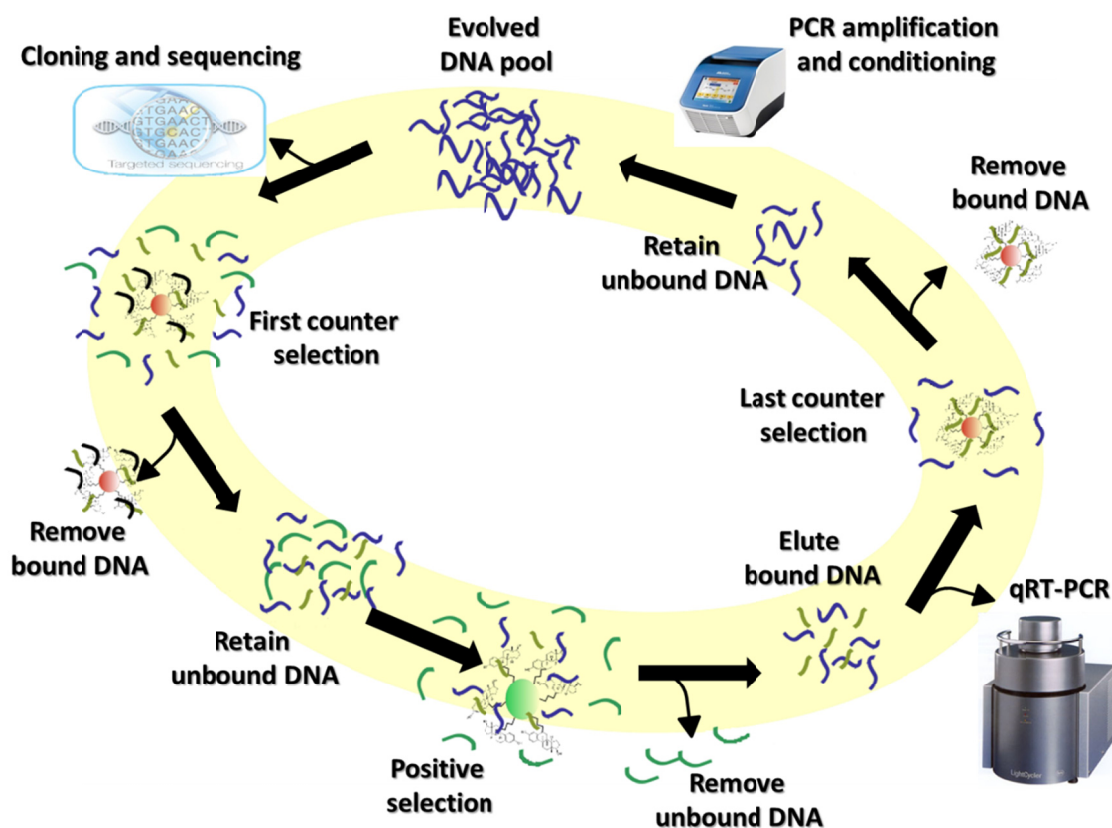


Figure 5: The optimized E2 SELEX procedure. Each SELEX cycle consists of two counter and one positive selection step, except the first cycle which consists of 6 counters and one positive. Red and green balls illustrate Sepharose beads attached to Nortestosterone and E2 molecules, respectively.

### 2.3.2 Counter selection step

The initial counter selection step was started by a random ssDNA library with around  $9.6 \times 10^{14}$  molecules. To this, 500  $\mu\text{l}$  of non-specific sonicated salmon sperm DNA (5 mg/ml) was added and it was evaporated at  $60^\circ\text{C}$  in a Concentrator plus (Eppendorf) until it was completely dry. The pellet was redissolved in 800  $\mu\text{l}$   $1 \times$  PBS containing 10% ethanol (PROLABO®). After a denaturation step on a shaking hot plate (Grant-bio, Cambridge, UK) at  $95^\circ\text{C}$  and 250-300 rpm, and a subsequent incubation on ice for 5 min, the solution was incubated with a fraction of blocked Nortestosterone beads for 1 hr at RT on a rotor. Transferring the solution containing unbound ssDNA to a new tube was done after centrifugation at 3200 rpm for 2 min. The collected solution from a single washing step of beads with 150  $\mu\text{l}$   $1 \times$  PBS containing 10% ethanol was added to the collected supernatant solution (total volume of 950  $\mu\text{l}$ ). Purification of the solution was performed through Sephadex™ G-50 Medium columns (GE Healthcare Biosciences, Uppsala, Sweden). After a complete evaporation, the sample was redissolved in 100  $\mu\text{l}$   $1 \times$  PBS containing 10% ethanol. At this point, 4  $\mu\text{l}$  of undiluted and a 1:100 diluted sample of the fraction were collected for sequencing and qRT-PCR purposes, respectively. It is important to note that after the last counter selection step of each cycle, instead of in  $1 \times$  PBS containing 10% ethanol, the sample was redissolved in 100  $\mu\text{l}$  of milli-Q water, because of inhibitory effects of ethanol on the subsequent PCR.

### 2.3.3 Positive selection step

In comparison to the counter selection step, the procedure of the positive step was exactly the same except for using E2 beads, extra washing steps, elution steps, and phenol-chloroform purification. After discarding the unbound aptamers, the E2 beads with the bound aptamers were washed five times with 300  $\mu$ l 1 $\times$  PBS for 3 min on a rotor at RT. Four elution steps were performed through the addition of 200  $\mu$ l preheated Tris/EDTA (TE) buffer containing 3 M urea pH 7.4 (10 mM Tris-Base, 2 mM EDTA, and 3 M urea) at 80°C on a hot plate shaking at 800 rpm for 5 min, and the supernatant of each washing step was collected. Phenol-chloroform purification was done on each elution fraction by the addition of 200  $\mu$ l phenol-chloroform isoamylalcohol (Sigma-Aldrich, Diegem, Belgium) to each tube, vortexing, and centrifuging at 13200 rpm for 3 min. The upper part of the resulting biphasic liquid, which contains the DNA, was collected into a new tube. This was repeated once again with 200  $\mu$ l chloroform isoamylalcohol (Sigma-Aldrich). After 2 Sephadex purifications for each elution fraction, the following sample preparation steps were exactly the same as during the counter selection.

### 2.3.4 qRT-PCR and second melting curve analysis

For the quantification of the molecule number, as well as for the determination of the enrichment of the selected aptamer molecules, qRT-PCR will be used. For quantification, the absolute amount of a known sequence in a sample is determined in the exponential phase of the DNA amplification. By using a fluorescent reporter in the reaction, it is possible to measure DNA synthesis. The DNA amplification is monitored at each elongation step of the qRT-PCR. When the DNA is in the logarithmic phase of amplification, the amount of fluorescence will increase above the background signal. The cycle at which the fluorescence becomes measurable is called the threshold cycle ( $C_T$ ) or crossing point. The more DNA that was present at the start of the reaction, the lower  $C_T$ . For the enrichment determination, the DNA will be amplified for 30 or more cycles. At the end of the amplification, by increasing the temperature, the dsDNA will denature and will result in a first melting curve. Decreasing the temperature will result in re-hybridization of the ssDNA sequences. This hybridization process is easier and faster for enriched fractions and produces more stable dsDNA structures than the hybridization of a complex, unenriched pool. Because of a high number of incorrectly re-hybridized dsDNA in random, unenriched fractions as compared to enriched ones, increasing the temperature again will result in a second melting curve which occurs at a lower temperature for unenriched fractions and at a higher temperature for enriched fractions. This effect is strongly dependent on the nature of the selected aptamers under certain conditions [25].

After the positive selection step of each SELEX cycle, 15.2  $\mu$ l of the 1:100 diluted fraction collected after the last counter selection step, and of the elution fractions of the positive selection step, were analyzed in a LightCycler (Roche) according to the program shown in table 3. The samples were compared with ssDNA library ladders containing  $10^{10}$ ,  $10^8$ ,  $10^6$  and  $10^4$  molecules and with a blank to determine the molecule number and the enrichment of the library. Apart from the DNA, the qRT-PCR reaction mix contained 2  $\mu$ l of SYBR-green (Roche), 2.4  $\mu$ l of 25 mM  $Mg^{2+}$  (Roche), 0.2  $\mu$ l of both 0.01 mM forward and reverse primers and milli-Q water up to 20  $\mu$ l. Depending on the molecule number and the difference in level of enrichment found in the four elution fractions of the positive selection step, the decision was made to continue the next step with a specific elution fraction or a combination of them. After selecting the elution fraction(s) to continue the SELEX process with, the molecule number of the sample was calculated based on qRT-PCR and 50 times more non-specific salmon sperm DNA was added to the sample. Then, the sample was evaporated completely and redissolved in 800  $\mu$ l 1 $\times$  PBS containing 10% ethanol for use in the next step.

Table 3: qRT-PCR program

Step	Number of cycles	Temperature (°C)	Time (min:s)	Temperature transition (°C/s)	Acquisition mode
Initial denaturation	1	95	10:00	20,00	None
Amplification	35-45	95	00:03	20,00	None
		54	00:05	20,00	None
		72	00:05	20,00	Single
Melting curve	1	95	05:00	20,00	Continuous
		72	01:00	20,00	Continuous
		95	00:00	0,10	Continuous
Cooling down	1	25	05:00	20,00	None

### 2.3.5 Amplification of the bound aptamers and generation of ssDNA to be used in the next SELEX cycle

After the last counter selection step, the remaining 95  $\mu$ l of library ssDNA in milli-Q water were divided into 5 PCR conditions. The PCR mix and program were exactly the same as the optimized condition described in section 2.2, except for using 0.01 mM phosphorylated reverse primer instead of unlabeled reverse primer, which is necessary for ssDNA generation. The number of amplification cycles varied between 20 and 25, depending on the earlier calculated molecule number of the library. All of the PCR product was run on a 4% agarose gel, and the lengths were compared with a 25 and 100 bp DNA length ladder. After analyzing the gel and recognizing the exact 80 bp band, it was cut out. Then, the chopped gel was soaked in crush and soak buffer pH 8.0 [500 mM  $\text{NH}_4\text{OAC}$ , 0.1% sodium dodecyl sulfate (SDS), and 0.1 mM EDTA] overnight at 4°C on a rotor. After centrifugation at 10000 rpm and collection of the supernatant, a single washing step with crush and soak buffer was performed on the gel remains, and the supernatant was added to the previously collected solution. Evaporation was performed to decrease the sample volume. Then, 1 phenol-chloroform and 2 Sephadex purifications followed as described in section 2.3.3. The concentration of dsDNA was determined by a NanoDrop 2000 spectrometer (Thermo Scientific, West Palm Beach, USA) with a peak at 260 nm wavelength.

The dsDNA was converted to ssDNA via Lambda exonuclease digestion. For this step, the sample was evaporated completely before 8.5  $\mu$ l milli-Q water, 1  $\mu$ l 10 $\times$  Lambda exonuclease buffer (Epicentre Biotechnologies, Madison, USA), and 0.5  $\mu$ l of 10 U/ $\mu$ l Lambda exonuclease enzyme (Epicentre) was added (for a concentration of dsDNA lower than 1 to 2  $\mu$ g). The mix was incubated at 37°C for 30 min on a hot plate (enzyme activation) and subsequently at 75°C for 10 min (enzyme deactivation). A Sephadex purification step was performed after increasing the volume to 40  $\mu$ l with milli-Q water. The concentration of ssDNA was determined by NanoDrop with a peak at 260 nm wavelength. After calculation of the ssDNA concentration, 100 times more non-specific salmon sperm DNA was added to the sample and evaporated completely. By redissolving the pellet in 800  $\mu$ l 1 $\times$  PBS containing 10% ethanol, the library was ready for the next SELEX cycle.

## 2.4 Sequence analysis

After a few SELEX cycles, collected fractions will be used for cloning into a plasmid vector, followed by transformation into bacteria, colony PCR and DNA sequencing of the aptamer inserts. Then, the sequences will be analyzed and compared, to check for the presence of identical aptamer sequences in different clones coming from different elutions. Repeated aptamer sequences from each elution will be selected as the specific aptamer for the target molecule [18, 20].

#### 2.4.1 TOPO vector cloning, transformation, and colony PCR

After finishing the 12<sup>th</sup> SELEX cycle, the fractions collected after the first counter selection step of cycle 10 and after the last counter selection step of cycle 12 were selected for cloning and sequencing. An amplification of 25 cycles was performed on these fractions according to the optimized PCR conditions described in section 2.2. This amplification increases the DNA concentration and it adds a single deoxyadenosine (A) to the 3'-end of the PCR products by the non-template-dependent terminal transferase activity of *Taq* polymerase, which is necessary for TOPO cloning. The PCR products were analyzed on a 4% agarose gel and the length was compared with a 25 and 100 bp DNA length ladder. For concentration analysis, samples were compared with a SmartLadder (Eurogentec, Seraing, Belgium) and the concentrations were analyzed with the aid of Quantity One<sup>®</sup> version 4.6.3 software. Confirmation of enough DNA for cloning was followed by making a cloning mix composed of 2 ng PCR product, 1  $\mu$ l salt (1.2 M NaCl, 0.06 M MgCl<sub>2</sub>) solution (Invitrogen), 1  $\mu$ l TOPO vector (Invitrogen) and milli-Q water up to 6  $\mu$ l. The mix was incubated at RT for 30 min.

Then, 2  $\mu$ l of cloned vector was added to a vial of One Shot<sup>®</sup> TOP10 chemically competent *E. coli* cells (Invitrogen) for transformation. After incubation of the mixture on ice for 30 min, the cells were given a thermal shock at 42°C while shaking at 700 rpm for 30 s and immediately kept on ice. Subsequently, 250  $\mu$ l pre-warmed Super Optimal broth with Catabolite repression (SOC) medium (Invitrogen) was added and incubated for 1 hr in a Stuart<sup>®</sup> shaking incubator SI500 (Bibby Scientific, Stone, UK) at 37°C with a speed of about 200 rpm. The transformation products were cultured on LB agar plates (Invitrogen) containing 100  $\mu$ g/ml Ampicillin (Invitrogen) and incubated at 37°C overnight.

Successful cloning and transformation was evaluated by colony PCR. Selected colonies were amplified for each fraction. In colony PCR, a colony was added to a 50  $\mu$ l PCR mix containing 5  $\mu$ l of 10 $\times$  PCR buffer, 1  $\mu$ l of 0.01 mM M13 forward primer (Invitrogen), 1  $\mu$ l of 0.01mM reverse primer (Invitrogen), 0.5  $\mu$ l of 20 mM dNTPs, 0.4  $\mu$ l of 5 U/ $\mu$ l *Taq* DNA polymerase, and 42.1  $\mu$ l milli-Q water. The PCR program is shown in table 4. Subsequent to the colony PCR, the concentration analysis with SmartLadder was done after separating the amplified products on a 2% agarose gel. The bands with a length of 280 bp (80 bp corresponding to the amplified aptamer sequence and 100 bp of the vector sequence flanking the aptamer on both sides) were known to contain the aptamer inserts.

Table 4: Colony PCR program

Process	Number of cycles	Temperature (°C)	Time
Initial Denaturation	1	95	5 min
Amplification	35	94	20 s
		55	20 s
		72	40 s
Final extension	1	72	6 min
Cool-down	1	4	$\infty$

#### 2.4.2 EXO-SAP-IT purification and sequencing

The PCR products were purified by EXO-SAP-IT (Affymetrix, High Wycombe, UK). Depending on the initial concentration of the PCR products, they were diluted or concentrated to 50 ng/5  $\mu$ l DNA in milli-Q water and 2  $\mu$ l of EXO-SAP-IT was added. The mixture was incubated at 37°C for 15 min (enzyme activation), followed by 80°C for 15 min (enzyme deactivation).

A sequencing PCR was done by adding 5  $\mu$ l of the purified product to 2  $\mu$ l of M13 forward primer, 2  $\mu$ l BigDye<sup>®</sup> buffer (Applied Biosystems, Warrington, UK) and 1  $\mu$ l BigDye<sup>®</sup> sequencing mix (Applied Biosystems) in a thermal cycler with the program as shown in table 5.

Table 5: Sequencing PCR program

Process	Number of cycles	Temperature (°C)	Time
Initial denaturation	1	96	5 min
Amplification	25	96	20 s
		50	20 s
		72	40 s
Cool-down	1	4	$\infty$

Then, the amplified products were again purified through Sephadex columns and evaporated completely. The pellet was resuspended in 25  $\mu$ l of Hi-Di<sup>™</sup> (Applied Biosystems) and kept at 95°C for 5 min followed by cooling on ice for 5 min to denature the products. Finally, the samples of each cycle were loaded onto an ABI PRISM<sup>®</sup> Genetic Analyzer 310 (Applied Biosystems) according to the optimized sequencing program (table 6).

Table 6: Sequencing program

Module	Injection time (s)	Injection voltage (kV)	Run voltage (kV)	Run temperature (°C)	Run time (min)
Seq. POP6 Rapid (1 ml)	20	2.0	15.0	50	36

### 2.4.3 Sequencing data analysis

The sequences were corrected using Chromas version 2.4.1 software and saved as a FASTA file. Then, the corrected sequences were analyzed and compared with Clustal-X version 2.1. Repeated sequences from each elution were selected and conformational analysis was done with the help of M-Fold [26] under the required conditions (Temperature: 25°C, Na<sup>+</sup>: 157 mM, Mg<sup>2+</sup>: 0 mM). Furthermore, composition and distribution of putative Quadruplex-forming G-Rich Sequences (QGRS) in the selected sequences were identified by the web-based QGRS mapper [27].

## 2.5 Affinity and specificity studies of selected aptamers via SPR

All the affinity and specificity studies of the selected aptamers were performed in a Biacore<sup>™</sup> T200 (GE Healthcare, Diegem, Belgium) system at 25°C with a four flow cell (FC) streptavidin (SA)-modified sensor chip (GE Healthcare). Biotinylated aptamer sequences and a BC-22 random ssDNA sequence were purchased from IDT (table 7). The random ssDNA sequence was selected since it had a different secondary structure in comparison with the selected aptamers, as defined by M-fold. Based on the secondary structure difference, it was assumed that the random sequence is not able to bind E2.

Table 7: The sequences of the biotinylated aptamers and BC-22 random ssDNA

Probe	Sequence
Aptamer sequence 1	5'-Biotin-TTT TTT TTG TGT GTG AGA CTT CGT TCC GGC GAT GGG GTA GGG GGT GTG GAG GGG CCG GAC GGA GGG GCA GCA AGG CAT CAG AGG TAT-3'
Aptamer sequence 2	5'-Biotin-TTT TTT TTG TGT GTG AGA CTT CGT TCC CCC GGT CGG TGG GGT AGG GGG CGT GGA GTC ACC GGG GGG GCA GCA AGG CAT CAG AGG TAT-3'
BC-22 random ssDNA sequence	5'-Biotin-TTT TTT TTT TAG CAG CAC AGA GGT CAG TTC GCC TGT AAG GTG GTC GGT GTG GCG AGT GTG TTA GGA GAG ATT GCC CTA TGC GTG CTA CCG TGA A-3'

### 2.5.1 SA-modified sensor chip immobilization

Via the immobilization wizard, the random ssDNA sequence was immobilized on FC 1 and 3 (reference flow cells), while the biotinylated aptamer sequences 1 and 2 were immobilized on FC 2 and 4 (active flow cells), respectively. The immobilization running buffer was 1× HPS-EP<sup>+</sup> (0.1 M HEPES, 1.5 M NaCl, 30 mM EDTA, and 0.5% v/v Surfactant P20) enriched with 350 mM NaCl. The immobilization wizard was composed of a preliminary washing step of all FCs with a solution containing 1 M NaCl and 50 mM NaOH and an immobilization step with 4 µl of 0.1 mM biotinylated sequences in 124 µl running buffer. Normalization of the detector was done with 70% glycerol (GE Healthcare). We aimed for an immobilization response of 2000 Response Units (RU) for all four FCs.

### 2.5.2 Affinity analysis of aptamers to E2

A serial dilution of E2 (Sigma-Aldrich) in 1× PBS containing 10% ethanol (0, 0.098, 0.195, 0.391, 0.781, 1.563, 3.125, 6.250, 12.500 and 25.000 µg/ml) was introduced to all the FCs of the immobilized sensor chip via a programmed wizard of the SPR system for small molecule studies. The method included a surface regeneration step with 5 mM NaOH, a washing step with 1× PBS containing 10% ethanol as running buffer, five start-up runs with running buffer, a first solvent correction step, all the E2 concentrations followed by a regeneration and washing step between each one, and a second solvent correction step. Duplicate measurements were performed for the E2 concentrations of 0 and 6.25 µg/ml. The flow rate and injection time were set at 60 µl/min and 120 s, respectively, while the dissociation time and stabilization time were both 60 s. The surface of the sensor that was saturated by target molecules was regenerated via the surface regeneration steps, while a solvent correction step was performed to allow to subtract the solvent effect of the samples from the response signal. Because 1× PBS containing 10% ethanol was the running buffer in this experiment, a sample series of 1× PBS containing a concentration range of ethanol between 9-11.6% was prepared for solvent correction (table 8).

Table 8: Solvent correction samples containing 1× PBS and different concentrations of ethanol

<i>Vial</i>	<i>1</i>	<i>2</i>	<i>3</i>	<i>4</i>	<i>5</i>	<i>6</i>	<i>7</i>	<i>8</i>
1× PBS + 9% ethanol (µl)	0	200	400	600	800	1000	1200	1400
1× PBS + 11.6% ethanol (µl)	1400	1200	1000	800	600	400	200	0
Total volume (µl)	1400	1400	1400	1400	1400	1400	1400	1400
Final ethanol percentage (%)	11.60	11.23	10.86	10.49	10.12	9.75	9.38	9.00

### 2.5.3 Specificity analysis of aptamers

Different cholesterol derivatives, including 17 $\alpha$ -ethinylestradiol, androstenedione, cholesterol, cortisone, deoxycholic acid, E2, estrone, and testosterone (all Sigma-Aldrich) were dissolved in 1× PBS containing 10% ethanol to prepare 6.25 µg/ml concentration, while a blank sample was used for each chemical. All the samples were introduced into all the FCs of the immobilized sensor chip according to the specifications in the small molecules method wizard. All the steps of the small molecules method wizard were as described in section 2.5.2, except for using only 2 different concentrations (blank and 6.25 µg/ml) per cholesterol derivative. All the measurements were performed in duplicate.

#### **2.5.4 SPR data analysis**

All the obtained SPR results were analyzed from real-time sensorgrams generated by the BIAevaluation 2.1 software. The sensorgrams were generated via subtracting the response of reference FC from active FC: FC 2-1 and FC 4-3.



### 3. Results and discussion

#### 3.1 PCR optimization of the ssDNA library

To have a reproducible amplification of the ssDNA library, PCR optimization was performed according to section 2.2. Based on the gradient PCR with 4 mM Mg<sup>2+</sup> and 10<sup>12</sup> molecules of random ssDNA library, different T<sub>a</sub>s were suitable, thus 54°C was selected to work with as a T<sub>a</sub> (figure 6). To obtain the best yield of products, 4 mM Mg<sup>2+</sup> and 10<sup>12</sup> DNA molecules were selected (T<sub>a</sub> = 54°C). Using 3 mM Mg<sup>2+</sup> and lower amounts of DNA, no bands were detected (figure 7).

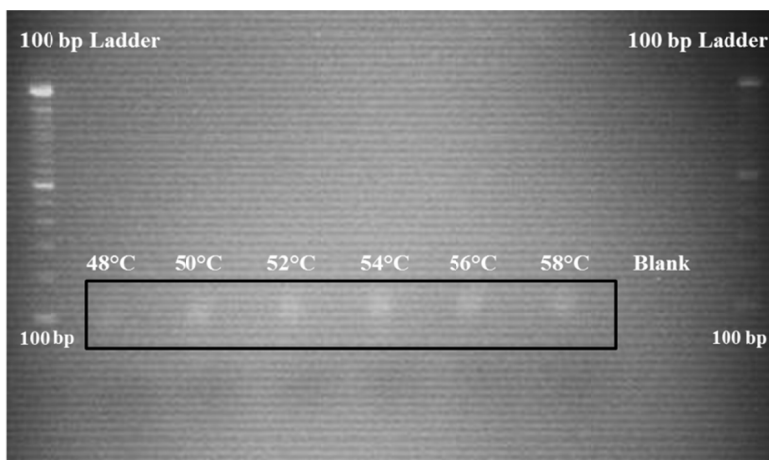


Figure 6: Gradient PCR products on a 3% agarose gel. From the temperature range 54°C was selected as the working T<sub>a</sub>.

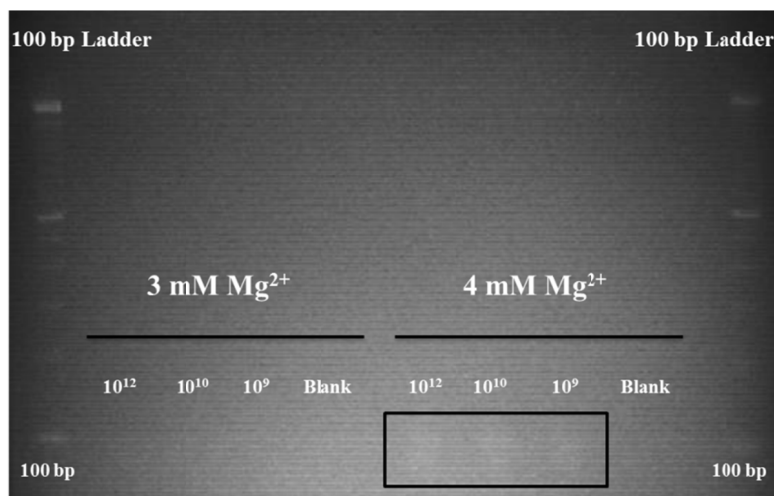


Figure 7: PCR products obtained with different input DNA, and 3 and 4 mM Mg<sup>2+</sup>. The highest amplification was obtained with 10<sup>12</sup> DNA molecules and 4 mM Mg<sup>2+</sup>.

#### 3.2 SELEX process and ssDNA library enrichment

The SELEX process was composed of 12 iterative cycles including positive and counter selection steps. Amplification and conditioning of the ssDNA library after each SELEX cycle were performed according to section 2.3.5. After the last counter selection step of each SELEX cycle, the library was amplified. The entire amplified library was run on a 4% agarose gel. Figure 8 shows a 4% agarose gel with a pure 80 bp band. The conditioning of the library was performed by cutting out the exact 80 bp

band and subsequent incubation of the gel band in crush and soak buffer. This was done to separate the actual aptamers from contaminant sequences, as well as artifacts (e.g. concatemers) of different lengths. Artifact sequences like concatemers can occur due to the fact that a high number of PCR cycles are necessary for SELEX process [20, 28].

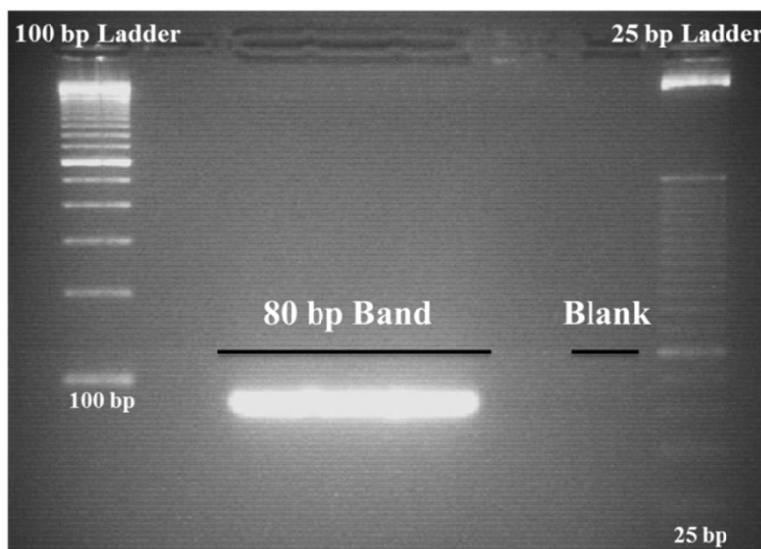
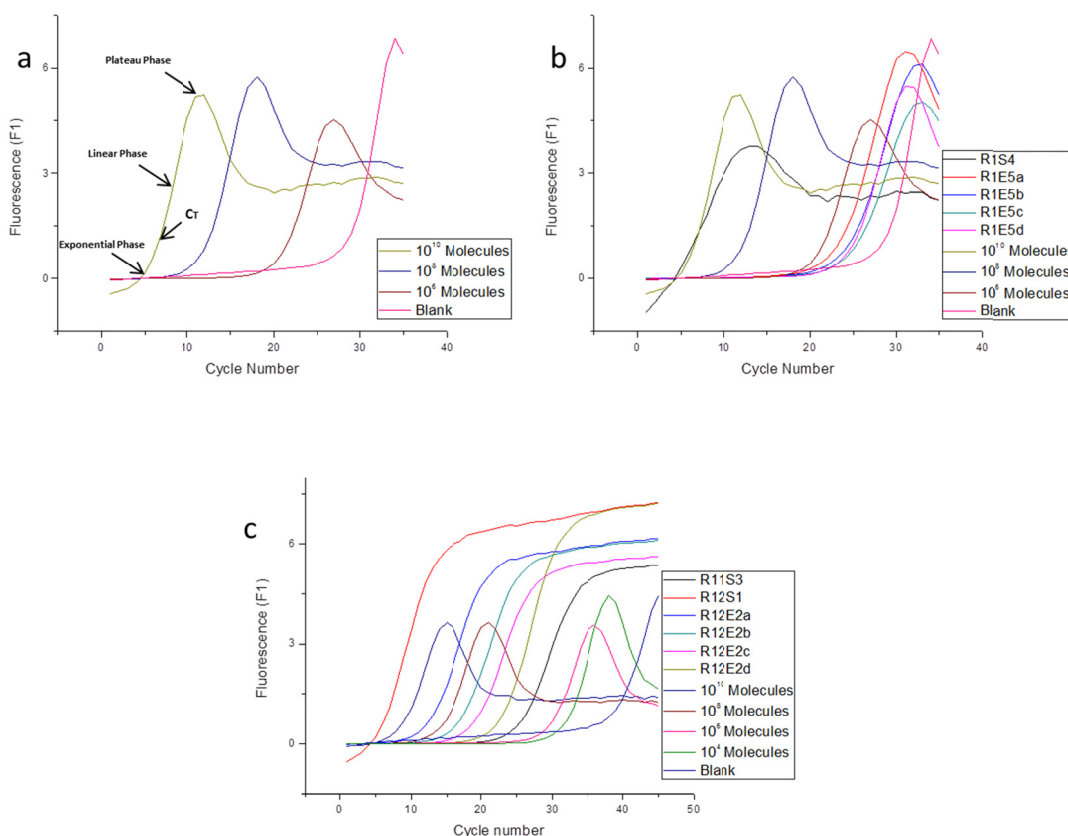


Figure 8: Conditioning of the library during SELEX. A 4% agarose gel with a pure 80 bp band after PCR.

As previously described in section 2.3.4, qRT-PCR and second melting curve analysis were used for the quantification and the assessment of enrichment of the selected aptamers during the SELEX, respectively [25]. All the collected fractions of the counter and positive selections were analyzed.

Figure 9a shows the fluorescence signal in function of the amplification cycle number for the ssDNA library ladders containing  $10^{10}$ ,  $10^8$ , and  $10^6$  molecules and a blank. The arrows determine the exponential phase,  $C_T$ , linear phase, and plateau phase in an amplification curve. Here, the shown plateau phase is not a real plateau, but shows a drop in fluorescence response. This drop is characteristic of the random ssDNA library, which will be explained later. The curves are nicely ordered according to the amount of DNA present, from  $10^{10}$  molecules having the lowest  $C_T$ , to the blank, containing only primers, having the highest  $C_T$ . As shown in figure 9b, molecule number estimation of all the SELEX fractions is possible by comparing their curves to the ladder and the blank. Normally, in each SELEX cycle, the first counter selection, the elution, and the last counter selection fraction will show a decreasing molecule number, which is logical due to deletion of some molecules after each selection step [20, 25]. Of the first cycle (R1), the 4<sup>th</sup> counter selection fraction (R1S4), as well as the 1<sup>st</sup> (R1E5a), 2<sup>nd</sup> (R1E5b), 3<sup>rd</sup> (R1E5c), and 4<sup>th</sup> (R1E5d) elution fraction are shown, together with the ladder and the blank of figure 9a. Estimation of the amounts of DNA molecules shows around  $10^{10}$  molecules in the R1S4 fraction, while the R1E5a, R1E5b, R1E5c, R1E5d fractions contain lower than  $10^6$  molecules. The elution fractions a and c have the highest and lowest molecule number, respectively, and both the b and d elution fractions, with similar molecule number, are placed in between. The distinctive shift to the right of the elution fractions in comparison to the counter selection fraction confirms the deletion of a large number of molecules unspecific to the target (E2) after the positive selection step [20]. It is important to note that, because of a lack of ladder accuracy, a ladder with  $10^4$  molecules was added from R2. Analyzing and comparing the patterns of cycle 12 curves (figure 9c) with those of cycle 1 curves (figure 9b), a significant transition is apparent from a fluorescence drop in the plateau phase in the 1<sup>st</sup> cycle to a smooth and gradual increase in the

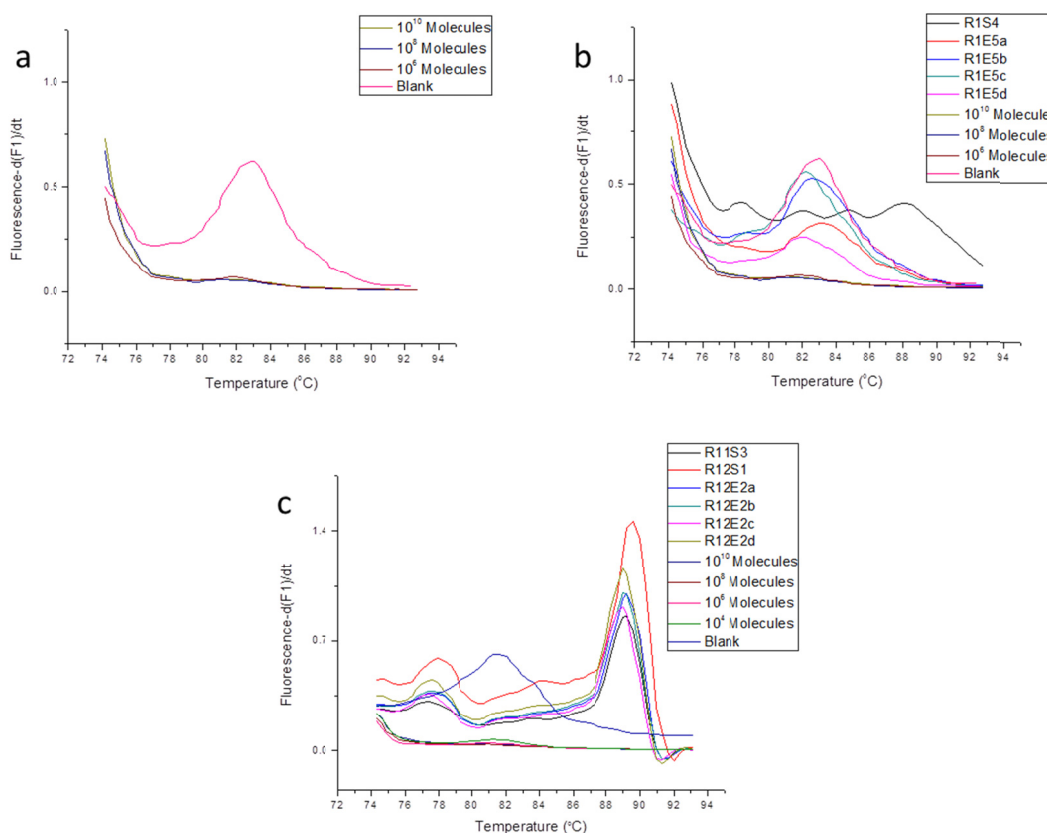
12<sup>th</sup> cycle. This change in the pattern of the amplification curves indicates the enrichment of the ssDNA library after the 12<sup>th</sup> SELEX cycle. At a certain moment during the amplification, dNTPs and primers run out, and the amplification stops in the reaction tube. However, the PCR program will still increase and decrease the temperature of the reaction tube. The decrease in temperature following the denaturation step results in a faster renaturation of the complementary strands, and hence a higher fluorescent response, in enriched fractions in comparison with the random library. In unenriched fractions, this re-hybridization occurs less efficiently, or not at all, resulting in a drop in fluorescence. The presence or absence of such a fluorescence drop can be used as an early indicator for enrichment in a ssDNA library, which is detectable sooner than by second melting curve analysis. In the present research, the fluorescent drop disappeared from the 6<sup>th</sup> cycle of SELEX, which indicates that the enrichment in the library has taken place (data are not shown).



Figures 9: Amplification plots of qRT-PCR of a) a DNA ladder containing  $10^{10}$ ,  $10^8$ , and  $10^6$  molecules, and a blank. Arrows show the exponential phase,  $C_T$ , linear phase, and plateau phase of the amplification. b) library fractions after the fourth counter selection step (R1S4) and all elution fractions (R1E5a, R1E5b, R1E5c and R1E5d) of SELEX cycle 1 (R1), together with the ladders and the blank. c) library fractions after the last counter selection step of SELEX cycle 11 (R11S3), as well as the 1<sup>st</sup> counter selection step (R12S1) and all elution fractions (R12E2a, R12E2b, R12E2c and R12E2d) of SELEX cycle 12, together with the ladders and the blank.

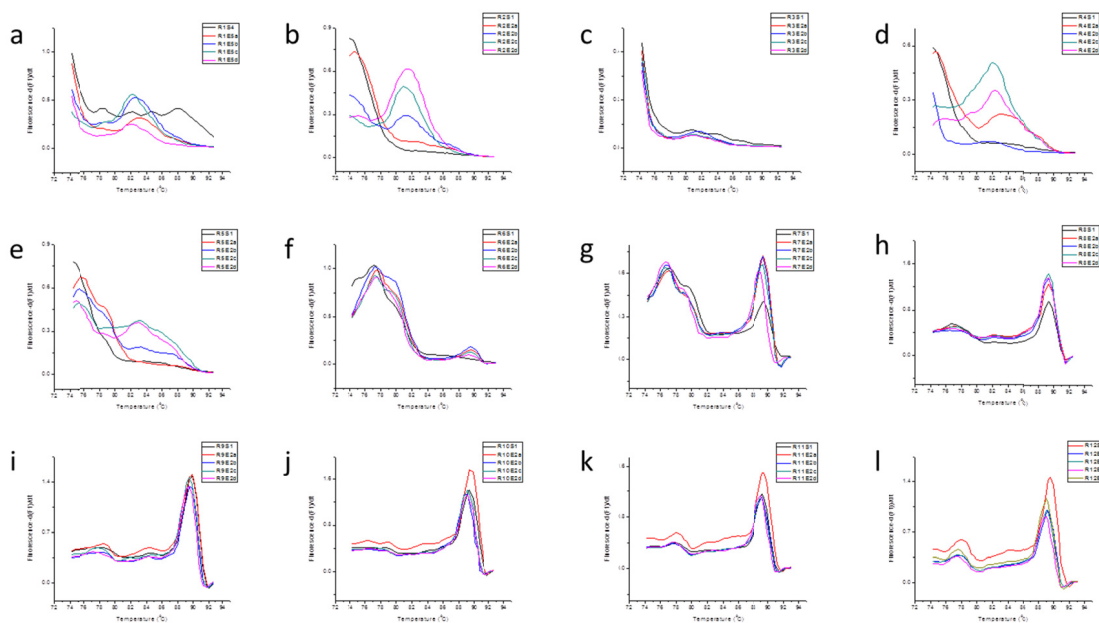
At the end of the amplification in qRT-PCR, second melting curve analysis was performed. Figure 10(a-d) shows the first derivative of the fluorescence response during the time ( $df1/dt$ ) in function of the temperature. Figure 10a shows the pattern of the ladder and the blank with a clear peak around 74°C. The blank sample also shows a clear peak at around 82°C, which is due to the denaturation of primer dimers. A peak comparable to the blank indicates a very low amount of DNA molecules in the

sample [29]. Comparison of the figures 10a and 10b confirms a random DNA library in the R1S4 and R1E5a-d fractions, with a peak at around 74°C for all fractions, and a peak at around 82°C for R1E5a-d, which resembles the denaturation of primer dimers due to a low amount of starting material. It is important to note that the blank also shows a small abnormal peak at 74°C, however this problem disappeared in subsequent cycles. The wave pattern of the 4<sup>th</sup> counter selection fraction of the first cycle (R1S4) between 76°C and 92°C can be due to an artifact. Comparison of the 1<sup>st</sup> and 12<sup>th</sup> cycle fractions (figures 10b and 10c) illustrates a transition in the peaks from a lower melting temperature at around 74°C for R1S4 and R1E5a-d fractions, to a higher melting temperature at around 89°C for R11S3, R12S1, and R12E2a-d fractions. This transition can be explained by the gradual decrease in the formation of mismatched or non-complementary duplexes when going from a random library in the 1<sup>st</sup> cycle to an enriched fraction in the last cycle. Increasing the number of complementary strands results in a melting curve at higher temperatures. A high melting temperature at around 89°C indicates a high level of enrichment. Disappearance of the primer dimer peak in R12 can be explained by a higher number of eluted molecules due to a stringent elution after the R12 positive selection step entered as qRT-PCR starting material. The small peak at 78°C can be explained by nucleotide mismatches due to *Taq* polymerase mistakes during amplification or to the presence of selected sequences with one nucleotide difference [30]. This effect will be explained more in section 3.3.



Figures 10: Second melting curve analysis of a) a DNA ladder containing  $10^{10}$ ,  $10^8$ , and  $10^6$  molecules, and a blank. b) library fractions after the fourth counter selection step (R1S4) and all elution fractions (R1E5a, R1E5b, R1E5c and R1E5d) of SELEX cycle 1 (R1), together with the ladder and the blank. c) library fractions after the last counter selection step of SELEX cycle 11 (R11S3), as well as the 1<sup>st</sup> counter (R12S1), and all elution fractions (R12E2a, R12E2b, R12E2c, and R12E2d) of SELEX cycle 12, together with the ladder and the blank.

Figure 11(a-l) illustrates the second melting curve analysis of the counter and 4 elution fractions of each SELEX cycle. The transition of the second melting curve peak from a lower to a higher temperature is clear after each cycle. The repeated pattern of cycle 1 and 2 in cycle 3 and 4 is because of a practical problem during the first and second cycle. Re-dissolving the library in  $1\times$  PBS containing 10% ethanol after the last counter step resulted in inhibition of the PCR reaction at the end of the SELEX cycle. According to Amita *et al.* any residual ethanol in the reaction mix may hinder the PCR as an inhibitor [31]. As mentioned in section 2.3.2, the problem was solved in the third cycle. A new random ssDNA library was regenerated by combining all the 4  $\mu$ l fractions collected after each selection step of the first two cycles. Cycle by cycle analysis and comparison of the peaks, indicate a transition in the melting temperature, which initially starts with a shift to the right as a shoulder pattern at 75°C during cycle 2 and 4, and it is changing to a clear peak at around 78°C in cycle 6. Also, during cycle 6 a small peak is starting to grow at around 89°C. As explained in the previous paragraph, this peak at 89°C can indicate the level of enrichment. From cycle 7 to cycle 8 the height of the left peak at 78°C decreased, while the height of the right peak at 89°C increased, due to the increase in the enrichment level. Furthermore, in cycle 9, the left peak disappeared completely and the right peak at 89°C was at the highest level, which logically confirms a high level of enrichment. To improve the enrichment level from cycle 9, a stringent positive selection step was applied. The stringent step was composed of lowering the quantity of E2 beads to half of the amount in comparison with previous cycles, as well as selecting the last elution fraction for amplification and continuing in next cycle. As a result of this stringent method a small change in the pattern of the second melting curve was detected in the appearance of a small peak at 78°C from cycle 9 to cycle 12, which is explained above.



Figures 11(a-l): Second melting curves of counter and elution fractions during SELEX. a) Cycle 1. b) Cycle 2. c) Cycle 3. d) Cycle 4. e) Cycle 5. f) Cycle 6. g) Cycle 7. h) Cycle 8. i) Cycle 9. j) Cycle 10. k) Cycle 11. l) Cycle 12. Transition of the melting temperature from 74°C to 89°C is visible during 12 iterative cycles.

### 3.3 Colony PCR, sequencing and data analysis

As described before (section 2.4), after TOPO vector cloning and transformation of the collected fractions of the 10<sup>th</sup> and 12<sup>th</sup> SELEX cycles, a colony PCR was performed on 56 selected colonies per

fraction, and on 5 untransformed, blank, colonies. Figure 12 shows a 2% agarose gel with bands at 280 bp for both SELEX cycles. The bands with 280 bp lengths confirm a successful sequence insert into the vector in contrast to the bands at around 200 bp without the sequence inserts, as can be seen in the blank colonies.

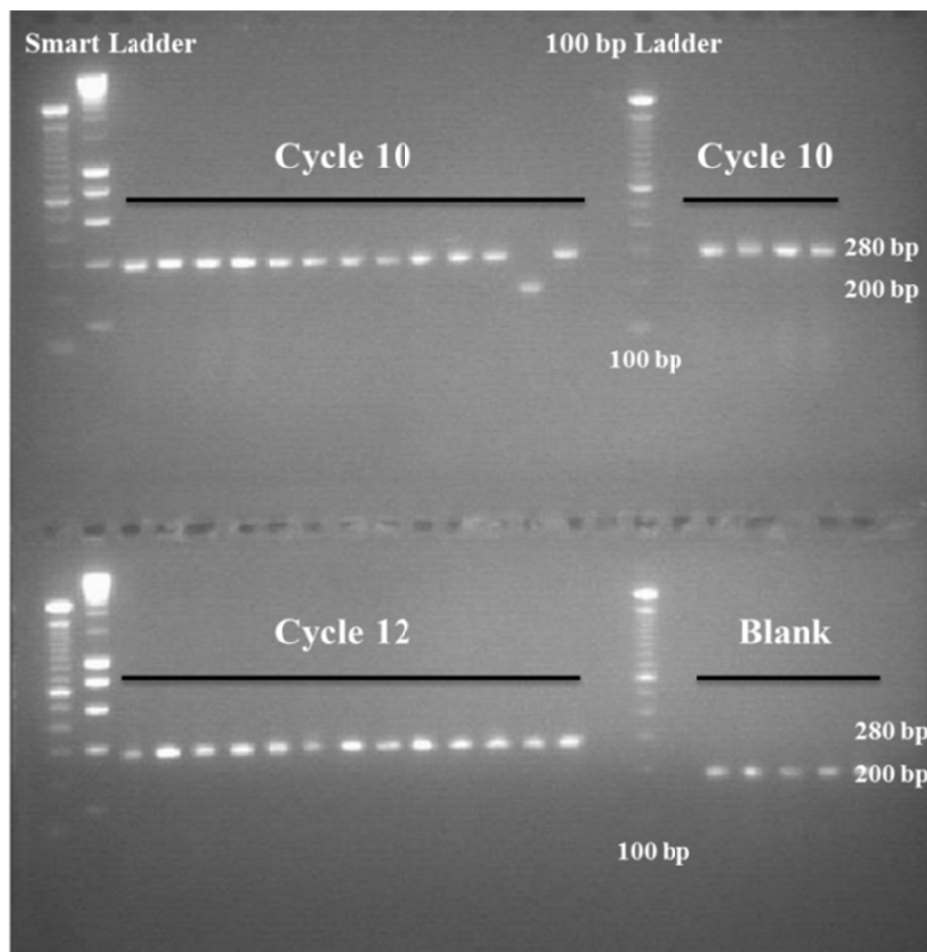


Figure 12: 2% agarose gel showing the products of the colony PCR to identify the aptamer bands of 280 bp in the collected selection and elution fractions of SELEX cycle 10 and 12.

In the next step, after sequencing 48 colony PCR products per fraction, the sequences were evaluated in Chromas version 2.4.1 software. The sequences were saved as FASTA files. All the FASTA files were analyzed and aligned in Clustal-X version 2.1. Figures 13a and 13b show all the aligned sequences of each SELEX cycle. Red and yellow boxes show repeated sequences in cycle 10 and 12, while purple and green boxes show the sequences that are uniquely linked to cycle 10 and 12, respectively.

Study of the aligned sequences of both cycles resulted in the detection of 4 different sequences, which were highlighted in red, yellow, purple and green in figure 13. According to table 10, sequences 1, 2 and 3, as well as sequences 1, 2 and 4 were found in cycle 10 and 12, respectively. Sequence 1 had the highest occurrence (81.3%) in the 48 sequences of cycle 12, while sequence 2 occurred highly in cycle 10 (79.2%). Sequence 3 and 4 were uniquely associated with cycle 10 and 12, respectively, and showed just one nucleotide difference in comparison with sequence 1 and 2, respectively. While the

fractions of cycle 10 and 12 were composed of a high number of both sequence 1 and 2, occurrence of sequences with a difference of just one nucleotide can be ascribed to *Taq* polymerase mistakes during

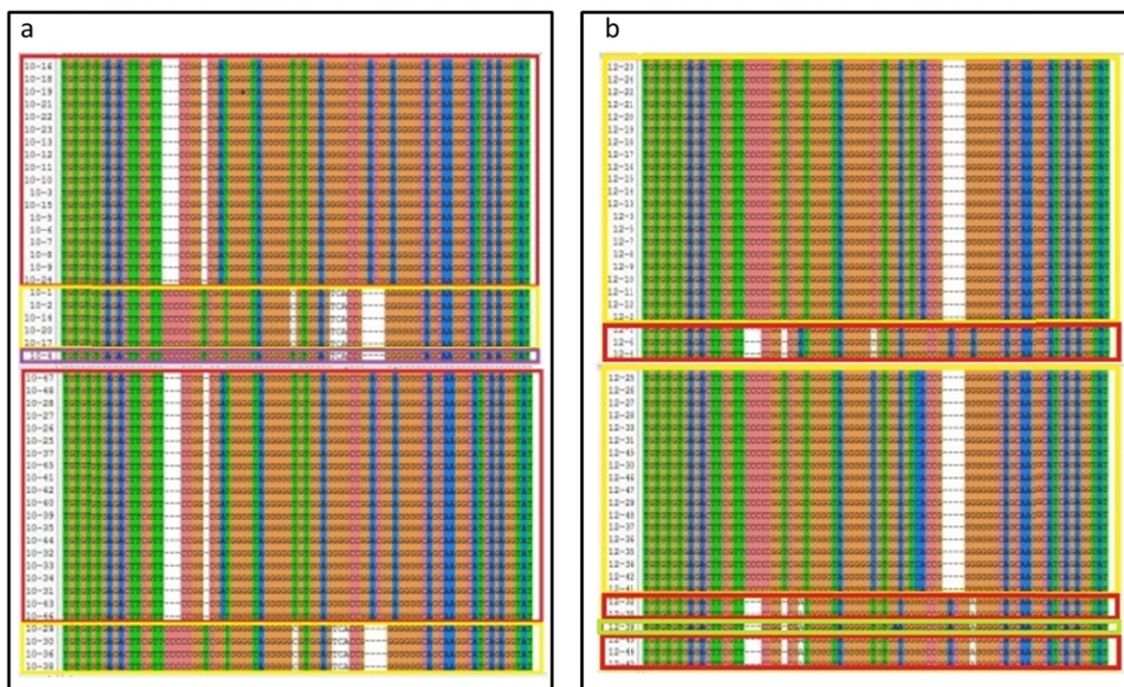


Figure 13: Sequence alignment in Clustal-X software of a) analyzed sequences of SELEX cycle 10. b) analyzed sequences of SELEX cycle 12. Red and yellow boxes show similar sequences in both cycles, while purple and green boxes show sequences uniquely linked to cycle 10 and 12, respectively.

the amplification step of PCR or sequencing [30]. Another hypothesis can be that these one nucleotide differences have specifically been selected for during the SELEX process. Anyhow, because of the low occurrence of sequence 3 and 4 in the selected SELEX cycles, most probably they are not aptamers with a good binding potential to the target. Therefore, they were not taken into consideration in the following studies and experiments.

Table 10: Four detected sequences in SELEX cycles 10 and 12, and their relative occurrence in each cycle. The red outer parts of the sequences show the primer binding sites. The nucleotides marked in purple mark the only difference between sequence 1 and 3, while those in green highlight the difference between sequence 2 and 4.

Number	Sequence	Occurrence in Cycle 10	Occurrence in Cycle 12
1	5'-TGT GTG TGA GAC TTC GTT CCC CCG GTC GGT GGG GTA GGG GG <sup>■</sup> GTG GAG TCA CCG GGG GGG CAG CAA GGC ATC AGA GGT AT-3'	18.8 % (9 out of 48)	81.3 % (39 out of 48)
2	5'-TGT GTG TGA GAC TTC GTT CCG GCG ATG GGG TAG GGG GTG TG <sup>■</sup> AGG GGC CGG ACG GAG GGG CAG CAA GGC ATC AGA GGT AT-3'	79.2 % (38 out of 48)	16.7 % (8 out of 48)
3	5'-TGT GTG TGA GAC TTC GTT CCC CCG GTC GGT GGG GTA GGG GG <sup>■</sup> GTG GAG TCA CCG GGG GGG CAG CAA GGC ATC AGA GGT AT-3'	2.1 % (1 out of 48)	0 % (0 out of 48)
4	5'-TGT GTG TGA GAC TTC GTT CCG GCG ATG GGG TAG GGG GTG TG <sup>■</sup> AGG GGC CGG ACG GAG GGG CAG CAA GGC ATC AGA GGT AT-3'	0 % (0 out of 48)	2.1 % (1 out of 48)

### 3.4 Conformational analysis

Conformational analysis of the selected sequences 1 and 2 was done with the help of the M-Fold server [26] under required conditions (Temperature: 25°C, Na<sup>1+</sup>: 157 mM, Mg<sup>2+</sup>: 0 mM). Figure 14 shows the obtained two-dimensional (2D) structure and specifications for sequence 1 and 2.

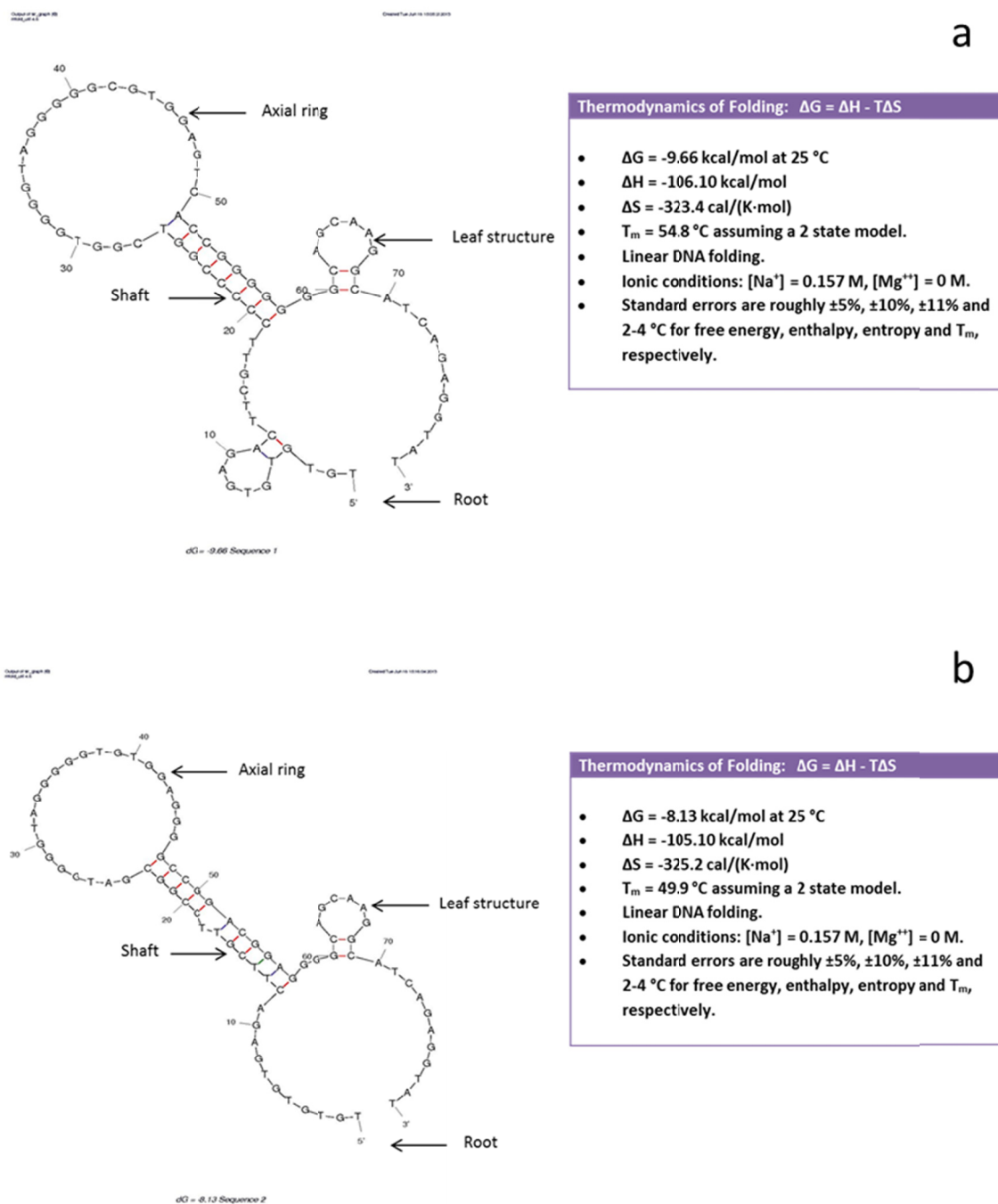


Figure 14: 2D structure and specifications for a) sequence 1, and b) sequence 2. Axial ring, shaft, leaf and root of the molecules are indicated by the arrows. The tables show the thermodynamic folding parameters for each molecule.

Conformational analysis under the desired conditions with the M-Fold server resulted in just 1 stable structure for both sequences. Thermodynamical comparison of both structures shows a little more stability for sequence 1 than for sequence 2 ( $\Delta G = -9.66$  versus  $-8.13$  Kcal/mol at  $25^{\circ}\text{C}$ , respectively).

Structural analysis of both sequences shows a highly comparable nucleotide pattern, especially at the 3' moiety. This similarity consists of a common free single-stranded sequence corresponding to the reverse primer binding site. The root of both molecules, composed of the 3' and 5' free parts, are joined to an axial ring by a shaft structure. The shaft is formed by the hybridization of the complementary sequences in the aptamer strand. The shaft structure of sequence 1 is shorter than that of sequence 2. A common leaf-shape structure is visible on the reverse primer binding sequence of both aptamers. However, another tiny leaf-shape structure is visible on the forward primer binding site of sequence 1.

Sequence analysis of both aptamers shows a high distribution of guanine (G) nucleotides. Different studies confirm that, because of a G-rich sequence in ssDNA molecules, the probability of a 3D G-quadruplex formation will increase. The G-quadruplex structure, also known as the G-quartet, is composed of stacked G-tetrads, which are square co-planar arrays of four G bases each. These highly stable structures can be formed by repeated folding of a single nucleic acid molecule and are generally very stable due to cyclic Hoogsteen hydrogen bonding between the four G bases within each tetrad (figure 15) [27].

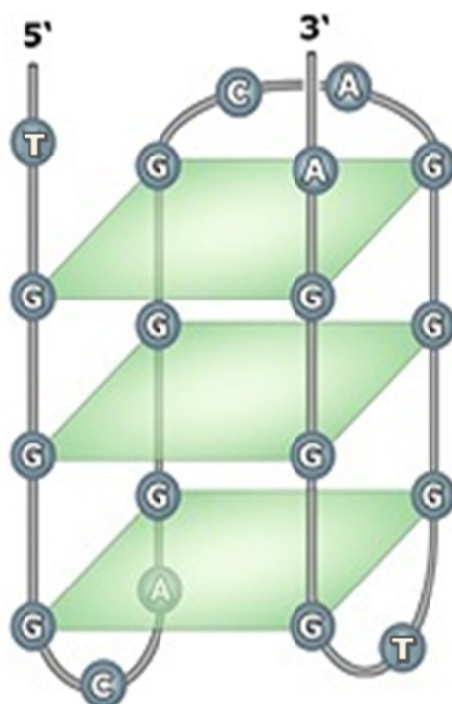


Figure 15: Predicted intramolecular G-quadruplex formed by a typical 'G'-Rich Sequence (5' TGGGCAAGGGCAAGGGTGGGA 3'). Square co-planar tetrads of four G bases are shown in green.

Screening for putative QGRS in sequences 1 and 2 was done with QGRS mapper. The web-based program evaluates the QGRS in a sequence for its likelihood to form a stable G-quadruplex by a scoring system (G-score). QGRS sequences with a higher G-score will make better candidates for G-quadruplexes. A G-score is calculated based on the potential number of G tetrads in the QGRS [27]. Table 11 shows the part of the sequence that is involved in quadruplex formation and its given G score for sequence 1 and 2. The obtained data for sequence 1 show a QGRS sequence with a length of 29 nucleotides and a G-score of 31. Two QGRS sequences of 29 and 21 nucleotides in length, which have a G-score of 21 and 14, respectively, were estimated for sequence 2. The number of G tetrads in the G-quadruplex is defined by the number of G bases in groups, which are outlined by boxes in QGRS sequence in table 11. Therefore, 3 G tetrads were detected for sequence 1, while 2 G tetrads were defined for both G-quadruplex possibilities of sequence 2. It is important to note that the greater the numbers of G-tetrads, the more stable the quadruplex, and the higher the G-score [27]. Thus, the quadruplex of sequence 1 is more stable than those of sequence 2. In another point of view, the position of the G groups involved in the quadruplex formation can be located in the M-Fold structure of each sequence. The positions of the G groups in sequence 1 are situated in the axial ring, shaft and reverse primer binding site. While, for the first possible G-quadruplex of the sequence 2, the groups are in the axial ring and shaft, and for the second possible G-quadruplex of the sequence 2, they are located in the reverse primer binding site and leaf structure.

Table 11: QGRS analysis for sequence 1 and 2(overlaps not included).

Sequence	Position (Nucleotide Number)	Length (Nucleotides)	QGRS Sequence	G-Score
1	32	29	GGG TAGG GGG CGTGGAGTCACC GGG GGGG	31
2	27	29	GGGGTAGGG GG TGTGGAG GG GCCGGAC GG	21
	57	21	GG GGCAGCAA GGCATCAGA GG	14

### 3.5 Affinity and specificity studies of the selected aptamers

Measuring the efficacy of the selected aptamers for E2 and their ability for specific binding to the target molecule is an important step in this thesis project. Attaining this goal is possible via affinity and specificity studies. Obtained results of these studies will direct the project to use the aptamers in the fabrication of a novel prototype E2 aptasensor. The Biacore SPR system is well suited to carry out qualitative studies to confirm the specificity of interactions as well as measurements for affinity, kinetics, and concentration determination [32, 33].

From the conformational studies and QGRS analysis of the selected aptamers described in section 3.4, it was apparent that the 3' ends of both selected sequences have a higher G-content than the 5' extremities, which possibly means that this part of the sequences is more involved in secondary structure formation and binding to the target molecule. For this reason, 5'-biotinylated versions of both aptamers were used for immobilization on SA-modified SPR sensor chips. Based on the Biacore Sensor Surface Handbook, an SA sensor chip is a glass slide coated with a thin layer of gold with a 3D-matrix of carboxymethylated dextran covalently attached to it (figure 16). To this dextran, SA is bound. SA can be used to capture biotinylated ligands with high efficiency. The affinity of SA for biotin is very high with a dissociation constant (KD) of around  $10^{-15}$  M [34], so that the ligand is in practice permanently attached to the surface.

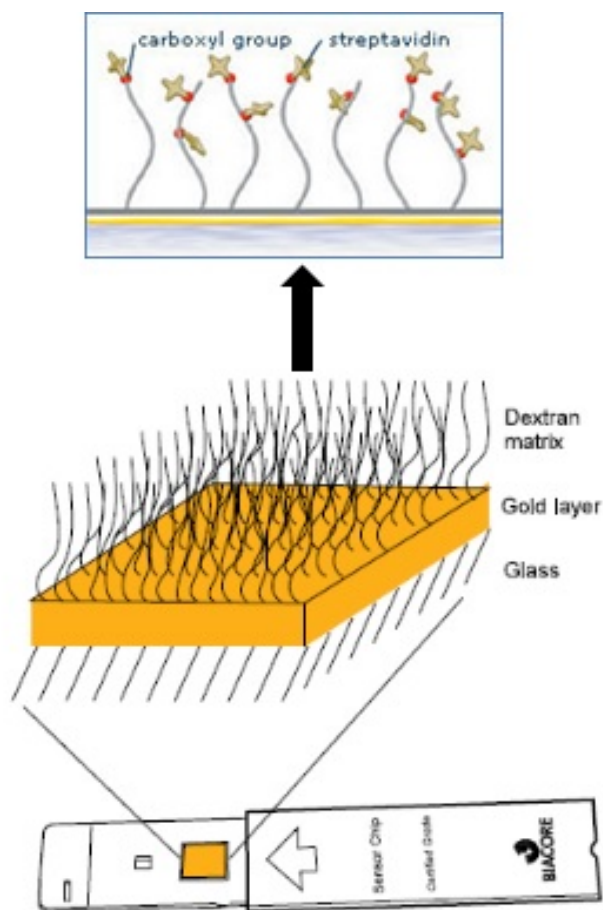


Figure 16: Schematic illustration of the structure of the SA sensor chip surface. A 3D-matrix of carboxymethylated dextran is covalently attached to a thin layer of gold. Onto this, SA molecules are attached, that serve as anchors for biotinylated ligands.

Successful immobilization of a biotinylated unspecific sequence (BC-22) on the reference FC 1 and 3, as well as biotinylated aptamer sequences 2 and 1 on the active FC 2 and 4, respectively, is shown in table 12. The targeted ligand response (RL) was set at 2000 RU. This value was selected based on the previous pilot studies on aptamers using SA chips. To explain the importance of the selected RL value on analyte concentration measurements, the Biacore Concentration Analysis Handbook illustrates that the analyte binding response for a given concentration seems to be related to the level of immobilized ligand, so that a high immobilization level can enable measurements of lower analyte concentrations. In addition, high levels of immobilized ligand ensure rapid binding of analyte and favor mass-transport limited binding, making concentration measurements less dependent on the affinity of ligand for analyte. On the other hand, the level of immobilized ligand may need to be kept lower in some cases. In the case of ligands such as aptamers, because they are large molecules and their binding ability is due to formation of their 3D structure on the surface, high levels of immobilized ligand (dense immobilization) can result in ligand crowding over the surface, and hence lack of space to make their secondary structure. This situation can limit the observed response, and hence the dynamic range due to a low number of active ligands. The analyte binding capacity of the ligand-functionalized surface will depend on the immobilization level and activity of ligand [5, 35].

The SPR response after analyte binding correlates with changes in mass concentration on the sensor chip surface, and therefore depends on the molecular weight (mass) of the analyte in relation to the number of ligand sites on the surface.  $R_{max}$  describes the maximum analyte binding response to the surface ligands in RU. The theoretical  $R_{max}$  is calculated from equation 1:

$$R_{max} = (\text{analyte MW/ligand MW}) \times RL \times S_m \quad \text{Equation 1}$$

where MW is the molecular weight (mass) of the ligand and analyte, RL is the amount of immobilized ligand in RU (ligand response), and  $S_m$  is the stoichiometry as defined by the number of binding sites on the ligand for the analyte [35]. The calculated theoretical  $R_{max}$  for active FC 2 and 4 were 19.89 and 20.34 RU, respectively (see table 12). The MW of analyte and ligand were 272 and 28710 Dalton (Da), respectively, and the stoichiometry was 1.

Table 12: Obtained RL after immobilizing all 4 FCs with either biotinylated unspecific ssDNA or aptamer sequences. The targeted response of 2000 RU was successfully reached for all 4 FCs.

<i>Ligand</i>	<i>RL (RU)</i>	<i>R<sub>max</sub> (RU)</i>
FC1 (BC-22)	2047.8	-
FC2 (Sequence 2)	2099.7	19.89
FC3 (BC-22)	1956.1	-
FC4 (Sequence 1)	2147.3	20.34

### 3.5.1 Affinity study of aptamers 1 and 2 for E2

An affinity study of the aptamers for the analyte E2 was performed via a pre-programmed small molecule method including solvent correction, as stated in section 2.5.2. Generally, when working with low molecular weight analytes dissolved in a solvent, to improve the response value, a solvent correction is necessary. Using solvents like ethanol in the buffer can result in a different response for the reference FCs in comparison to the active FCs. The effect of the solvent on the reference FC, which probably has more empty spaces, is totally different than on an active FC without any or with less empty spaces. Based on the suggested protocol for a Biacore system by the company, to check if this solvent effect takes place, different concentrations of the solvent are run over the chip during the solvent correction cycles. If there is no difference between reference and active FCs, and so no solvent effect, the actual reference response value will be around zero, and no correction is necessary. However, when a solvent effect exists, the actual reference response value is different from zero, so correction is necessary. The concentrations used are summarized in table 8. Figure 17 shows the first and second solvent correction step for FC 2-1 and FC 4-3. Subtraction of the response of the reference FCs, or the blank, from that of the corresponding active FCs (actual response) helps to eliminate systematic variations in the response and improves the robustness of the assay. Curves in blue and purple refer to FC 2-1, while the green and gray ones refer to FC 4-3, for solvent correction step 1 and 2, respectively. Both solvent correction steps for FC 2-1 show a regular response pattern around zero with increasing ethanol concentration. The responses for FC 4-3 are disordered and deviated from zero, and the curves of both solvent correction steps are not similar. Response values around zero for similar curves of FC 2-1 seem logical, since the reference and the active FCs are occupied by either unspecific ssDNA or aptamer sequences, respectively. Thus, the open spaces for both types of FC are probably equal, and as a result the solvent effect on both FCs will be the same. Although analogous results were expected for FC 4-3, the results, which show responses deviating from zero with non-conforming curves, can be explained by an artifact due to delayed measurement of the response of the

same solvent sample in serial FCs. The vertical lines in figure 17 indicate that all the measured response values of the E2 samples are situated in between of these two lines, which indicates that all measured values are in the solvent correction range (9-11.6%). This fact confirms that all E2 samples were dissolved in 10% ethanol, correctly.

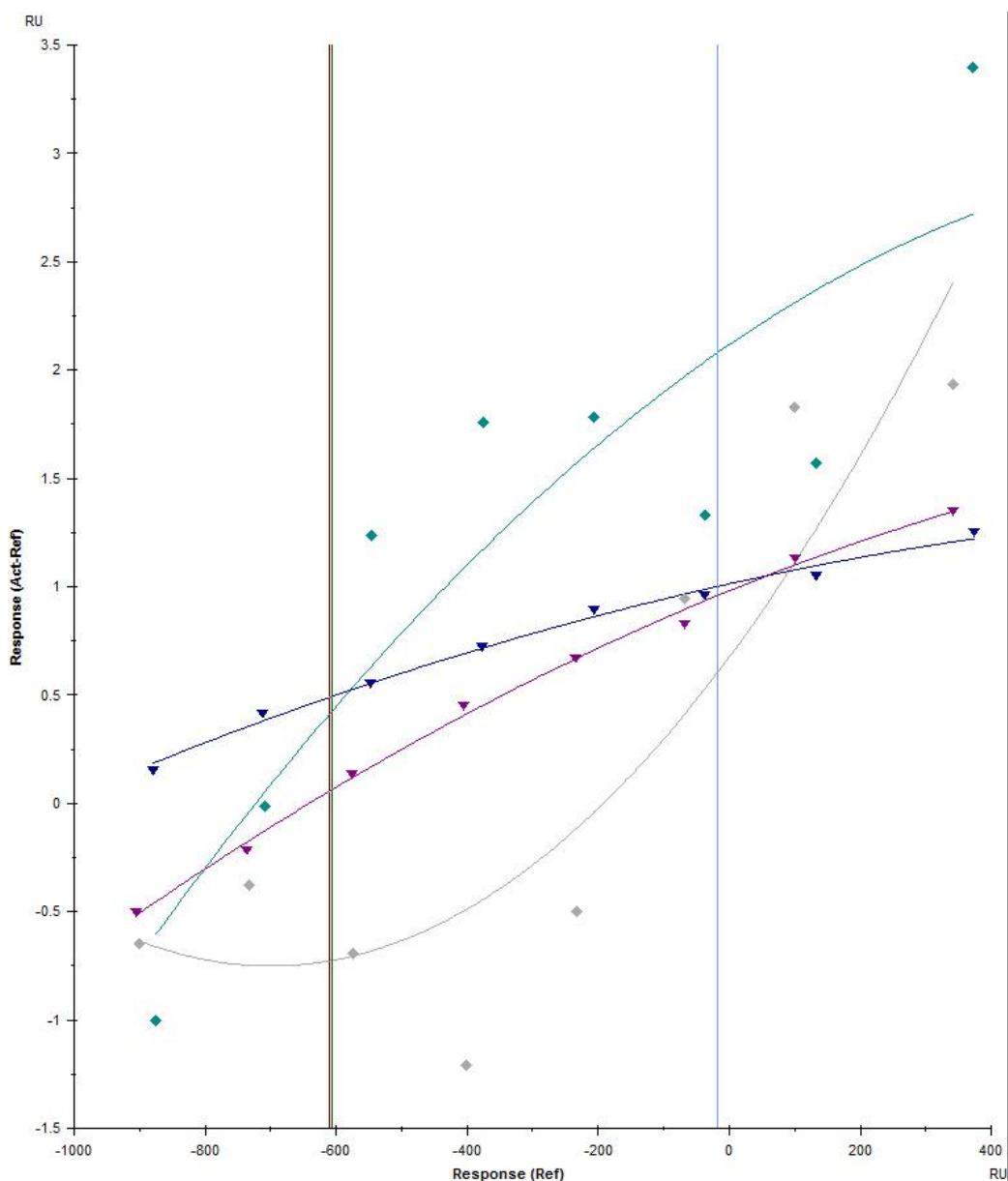


Figure 17: First and second solvent correction steps for FC 2-1 and FC 4-3. Blue and purple refer to FC 2-1, while green and grey refer to FC 4-3, for the first and second step, respectively.

Typically, a kinetics or affinity study determines whether a ligand-analyte complex forms or dissociates within a certain time span. The kinetics of a reaction is described by association ( $K_a$ ) and dissociation ( $K_d$ ) rate constants.  $K_a$  is referred to as the rate at which a complex is formed, while  $K_d$  is the rate at which a complex dissociates. Affinity indicates how much ligand-analyte complex is formed at equilibrium, which gives an idea about the complex strength or stability. When the association and dissociation rates are too fast, which often is the case for small molecules, calculation of these kinetic rate constants is not possible. The equilibrium dissociation constant or affinity

constant ( $K_D$ ) is the propensity of a ligand to separate (dissociate) from an analyte molecule at equilibrium conditions.  $K_D$  is used to describe the affinity between a ligand and an analyte, i.e. how tightly a ligand binds to an analyte, which is inversely proportional to the equilibrium association constant ( $K_A$ ). A ligand with a lower  $K_D$  has a higher affinity for the analyte (stronger binding). Rate constants can provide a link between ligand function and structure, e.g., in the evaluation of the impact of nucleotide substitutions on the interaction between aptamer and target.  $K_D$  values can be derived either from interactions that have reached equilibrium, or from the ratio of the dissociation and association rate constants ( $K_D = K_d/K_a$ ) in cases where the system does not reach steady-state during the time frame of the experiment. The typical working range for affinity measurements with a Biacore system is picomolar to high micromolar  $K_D$ s. Association rate constants can be measured ranging from  $10^3$  to  $10^8 \text{ M}^{-1} \text{ sec}^{-1}$  and dissociation rate constants from  $10^{-5}$  to  $1 \text{ M}^{-1} \text{ sec}^{-1}$  [32, 33, 35, 36].

Solvent-corrected measurements for different concentrations of E2 showed a saturation state of the aptamer-modified sensor surface at E2 concentrations of more than  $3.125 \mu\text{g/ml}$  for FC 2-1 (aptamer sequence 2), and  $6.25 \mu\text{g/ml}$  for FC 4-3 (aptamer sequence 1) (data not shown). Figure 18 shows the solvent-corrected and blank-subtracted graph of an E2 concentration range from  $0.098$  to  $6.25 \mu\text{g/ml}$  for sequence 2. A dose-dependent increase of the E2 response is obvious for E2 concentrations lower than  $3.125 \mu\text{g/ml}$ , while the lowest detectable E2 concentration was  $0.098 \mu\text{g/ml}$ . The almost similar response for  $3.125$  and  $6.25 \mu\text{g/ml}$  of E2 can be explained by reaching the saturation point of the sensor.

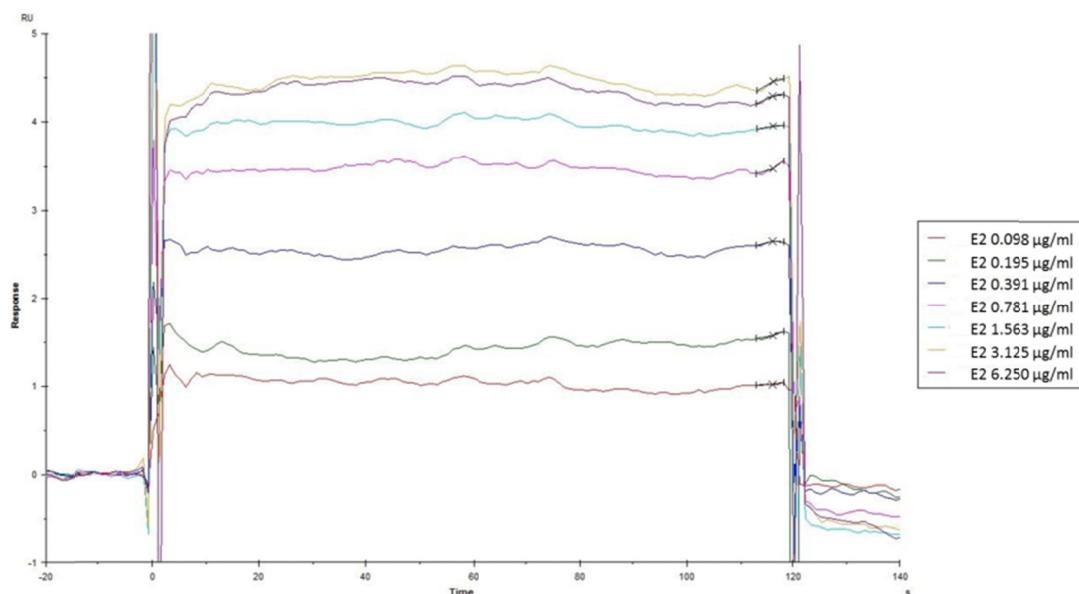


Figure 18: Solvent-corrected and blank-subtracted graph of an E2 concentration range from  $0.098$  to  $6.25 \mu\text{g/ml}$  for sequence 2.

Considering the fact that the entire binding cycle is repeated for each concentration of analyte, it can be used to generate a robust data set for global fitting to an appropriate binding algorithm. As previously described, in this case the affinity of the interaction cannot be calculated from the ratio of the rate constants ( $K_D = K_a/K_d$ ), because of a very fast  $K_a$  and  $K_d$  for small molecules. The solution for measuring  $K_D$  is to make a fitting of the response at equilibrium at varying concentrations of analyte. The  $K_D$  is equal to the concentration of analyte that gives half of  $R_{max}$  [37]. Global fitting of

the responses for different E2 concentrations for FC 2-1 is shown in figure 19. The calculated KD (the intersection point of the vertical line and the curve) for the aptamer sequence 2 was 0.947  $\mu\text{M}$  at an actual  $R_{\text{max}}$  of 5.136 RU with a good Chi-square of 0.026. The Chi-square shows the adequacy of the global fitting test. A good global fitting is indicated by a Chi-square lower than 10% of the  $R_{\text{max}}$  [36].

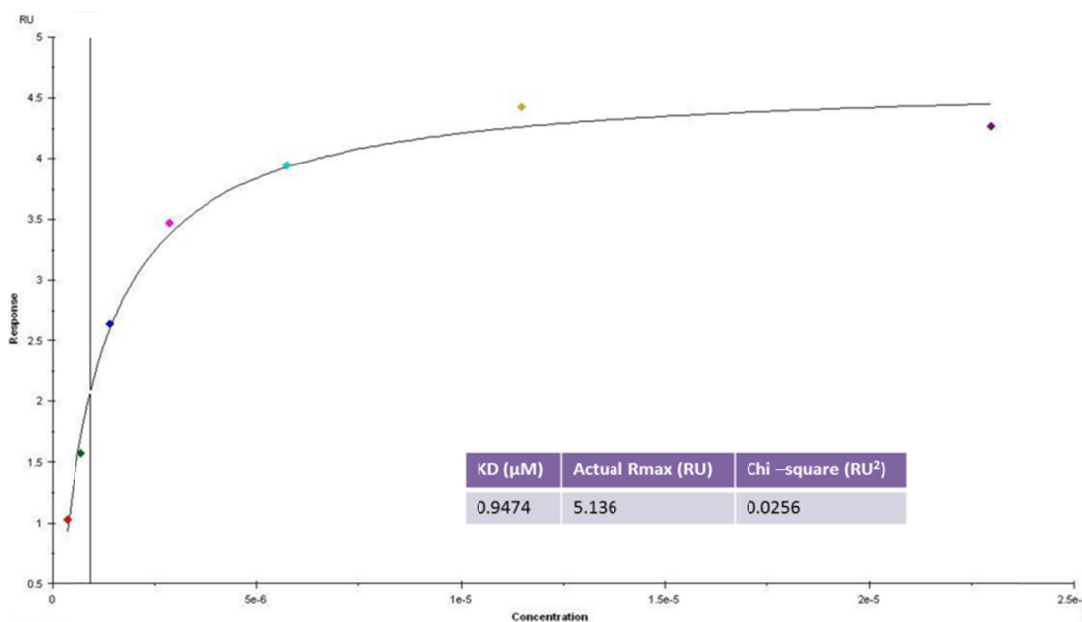


Figure 19: Global fitting of the responses for different E2 concentrations for sequence 2. The Chi-square is 0.026.

Figure 20 shows the solvent-corrected and blank-subtracted graph of the same E2 concentration range for sequence 1. According to the figure, the lowest detectable E2 concentration was 0.391  $\mu\text{g/ml}$ , which is logical due to the lower affinity of sequence 1 that will be described in this paragraph. A dose-dependent increase of E2 response is obvious for E2 concentrations higher than 0.391  $\mu\text{g/ml}$ . Based on the fitted responses in figure 21 the KD for aptamer sequence 1 was calculated to be 7.666  $\mu\text{M}$  at an  $R_{\text{max}}$  of 2.891 RU with a good Chi-square of 0.008. The lower KD for aptamer sequence 2 in comparison to sequence 1 (0.947 vs. 7.666  $\mu\text{M}$ , respectively) indicates a higher affinity of sequence 2 to E2. In comparison, the lower  $R_{\text{max}}$  for sequence 1 as compared to sequence 2 (2.891 vs. 5.136 RU, respectively) shows a lower sensitivity compared to sequence 2. This indicates that, although sequence 1 has the highest occurrence after applying the stringent elution in cycle 12 (table 10) and it was expected to have higher sensitivity and affinity than sequence 2, it seems that overselection under stringent elution resulted in an aptamer with lower sensitivity and affinity, at least under the applied condition (e.g. temperature, and flow rate) of the affinity study. Also, the lower actual  $R_{\text{max}}$  for both FC 2 and 4, in contrast to the calculated theoretical  $R_{\text{max}}$  in section 3.5 (5.136 vs. 19.89 RU, and 2.891 vs. 20.34 RU, respectively), can be ascribed to a higher unspecific binding of E2 to the reference FCs than to the active FCs due to a higher sample speed in the reference FC than in the active FC because of the serial piping system of SPR. Also, another reason can be lower numbers of active ligands on the surface of the active FCs due to a dense immobilization as suggested by Kim *et al.* [5]. As described before in section 3.5, because of a dense immobilization on the sensor surface, aptamers may not have enough space to fold and make their secondary structure, necessary for analyte binding.

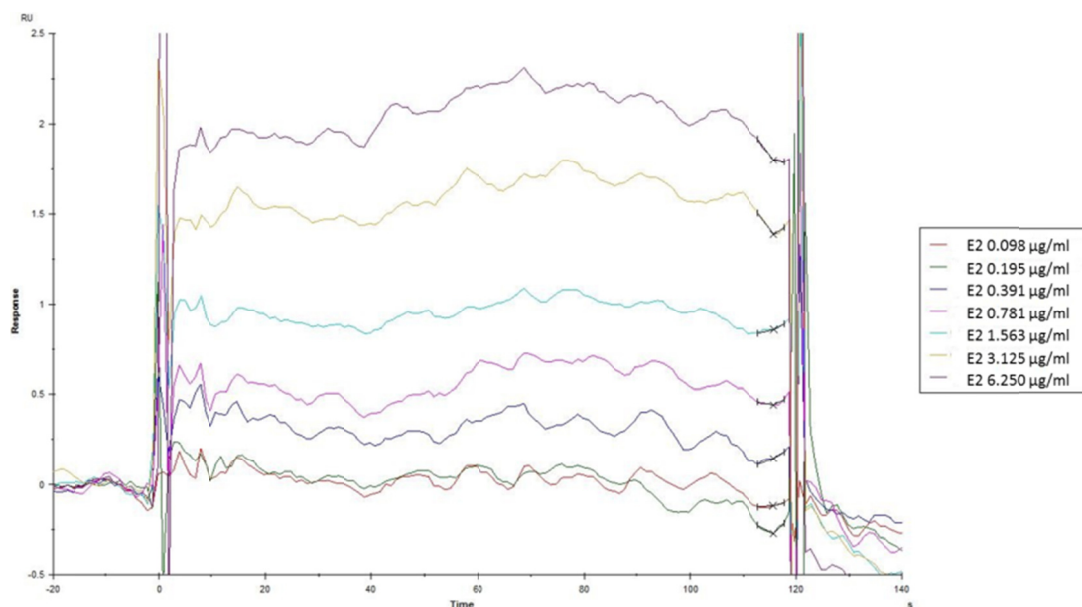


Figure 20: Solvent-corrected and blank-subtracted graph of an E2 concentration range from 0.098 to 6.25  $\mu\text{g/ml}$  for sequence 1.

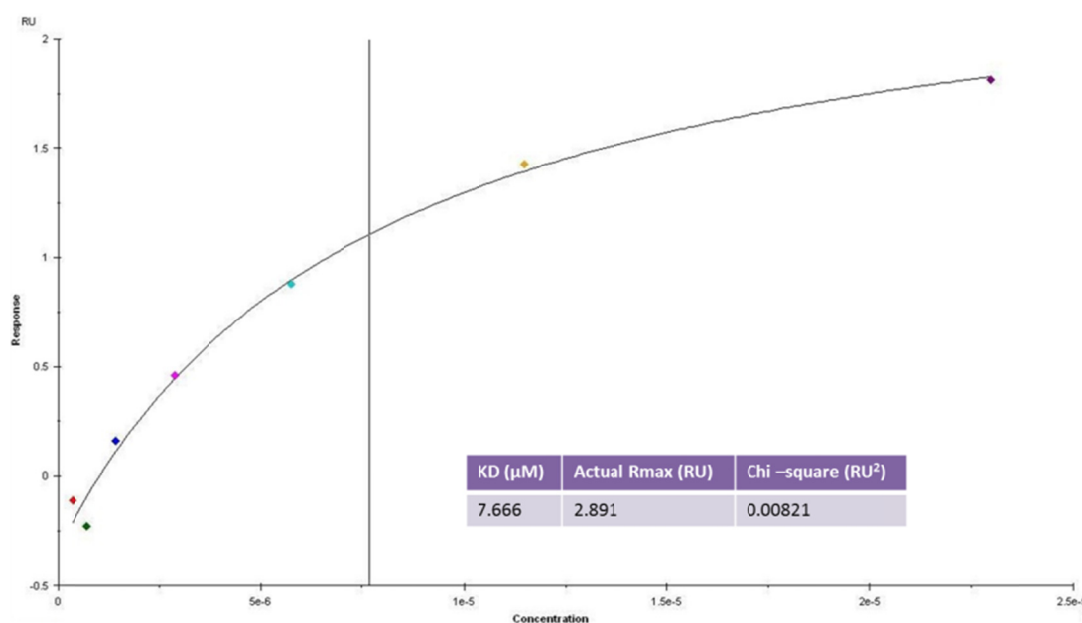


Figure 21: Global fitting the responses for different E2 concentrations for sequence 1. The Chi-square is 0.008.

Since no SPR-based aptasensor has been reported similar to this project, the obtained results of this experiment can be compared with the results of Kim *et al.* They selected a 76-mer ssDNA aptamer showing a KD of 0.13  $\mu\text{M}$  based on an equilibrium-filtration method. Comparing the KD values indicates that the KD of their aptamer was around 7.5 and 60 times lower than the calculated KD for sequence 1 and 2, respectively (0.13 vs. 0.947 and 7.666  $\mu\text{M}$ ). This lower KD confirms a higher affinity of their aptamer than both selected aptamers in this project. As the next step, they immobilized their aptamer on an SA-modified gold electrode to develop an electrochemical E2

aptasensor. With Cyclic Voltametry (CV) and Square Wave Voltametry (SWV), they reported a linear range of detection of E2 in the concentration range 0.01-1 nM (0.00001- 0.01 $\mu$ M) [5]. In the present research the concentration ranges were 0.098-3.125  $\mu$ g/ml (0.36-11.47  $\mu$ M) and 0.391-6.25  $\mu$ g/ml (1.44-22.95  $\mu$ M) for sequence 2 and 1, respectively. Comparing the calculated concentration ranges of this research project with the Kim *et al.* results confirms a broader detection range for E2 in the present aptasensor utilizing either sequence 1 or 2 in comparison to their aptasensor. However, their aptasensor was working in nM range (higher sensitivity), but the present setup is working in  $\mu$ M range.

It is important to note that Kim's group attempted to fabricate an SPR-based aptasensor, but that their selected aptamer was unsuccessful. They specified that their Biacore 3000 system, with a 400 Da cut-off, cannot produce a signal for the small E2 molecule with a molecular weight of 272 Da [5], while in this project a Biacore T200 system was used, which is more sensitive to molecules smaller than 400 Da. However, efforts of the biosensor group of Hasselt University in using the Kim *et al.* aptamer on the Biacore T200 were also unsuccessful, which can be explained by the unclear working condition of their aptamer.

### 3.5.2 Specificity study of different cholesterol derivatives

As previously described in section 2.5.3, specificity studies of aptamers for E2 and other cholesterol derivatives were performed via a small molecule method containing solvent correction cycles. The chemical structures of E2 and other cholesterol derivatives used in this study, as well as Nortestosterone, are shown in figure 22.

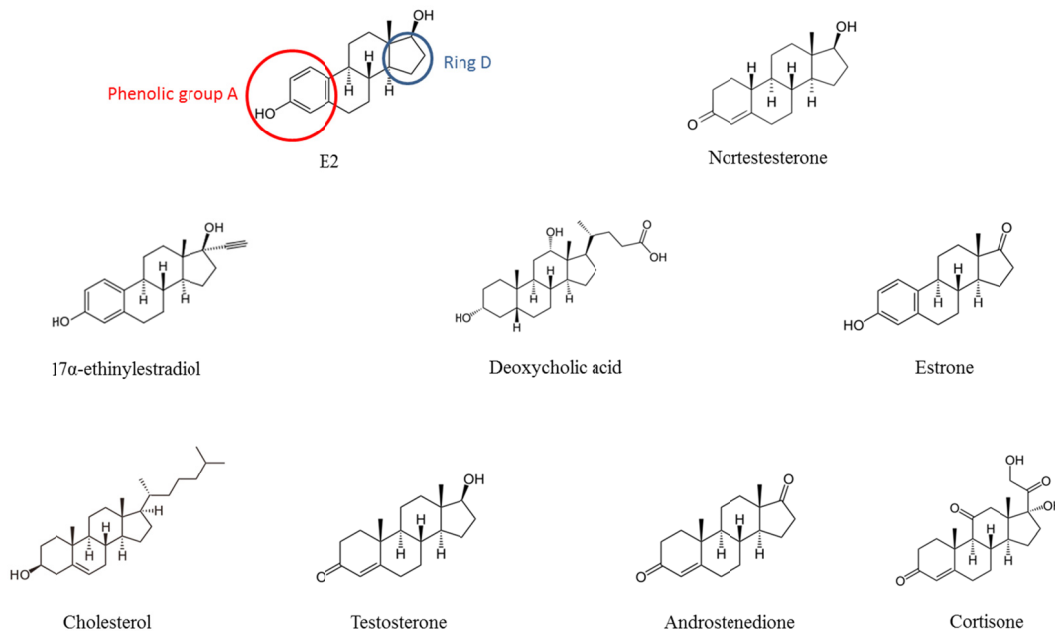


Figure 22: Chemical structures of E2 and other cholesterol derivatives used in this study. The phenolic group A and ring D are shown with red and blue circles in the E2 molecule, respectively.

The solvent-corrected and blank-subtracted relative response at 5 s before the end of analyte injection (binding late) for E2 and cholesterol derivatives to sequence 2 is shown in figure 23. The highest binding responses were detected for 17 $\alpha$ -ethinylestradiol, E2 and Estrone, with a maximum of around

4 RU for 17 $\alpha$ -ethinylestradiol. The maximum responses for other chemicals were lower than 1 RU. Comparative results were obtained for sequence 1, with the maximum binding response around 2.5 RU for 17 $\alpha$ -ethinylestradiol (figure 24). Again, lower maximum binding responses of sequence 1 compared to sequence 2, confirms its lower sensitivity.

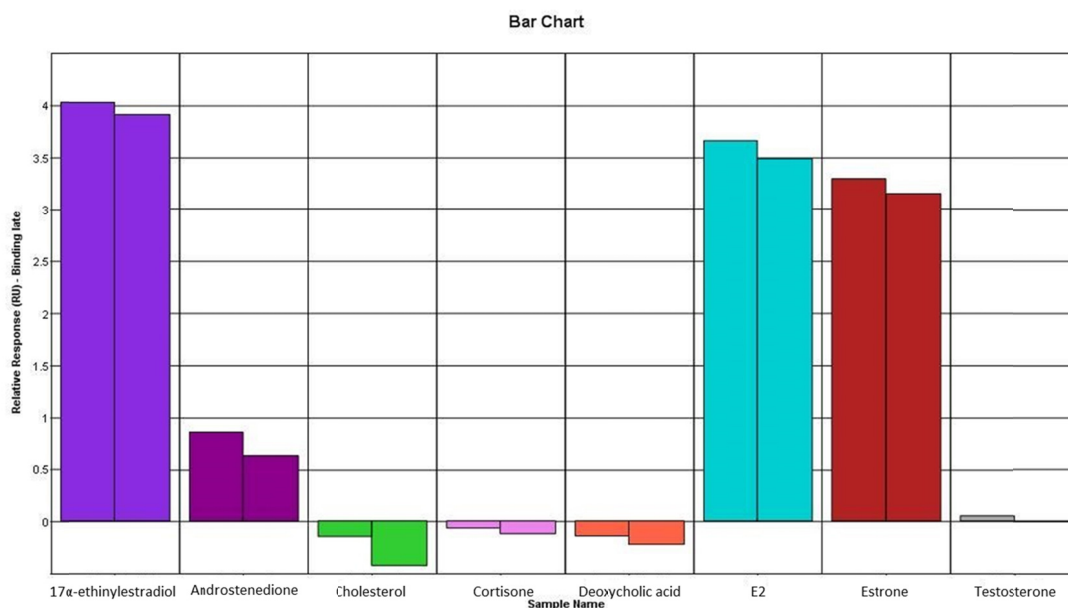


Figure 23: Solvent-corrected and blank-subtracted relative binding responses of E2 and structurally related cholesterol derivatives to sequence 2.

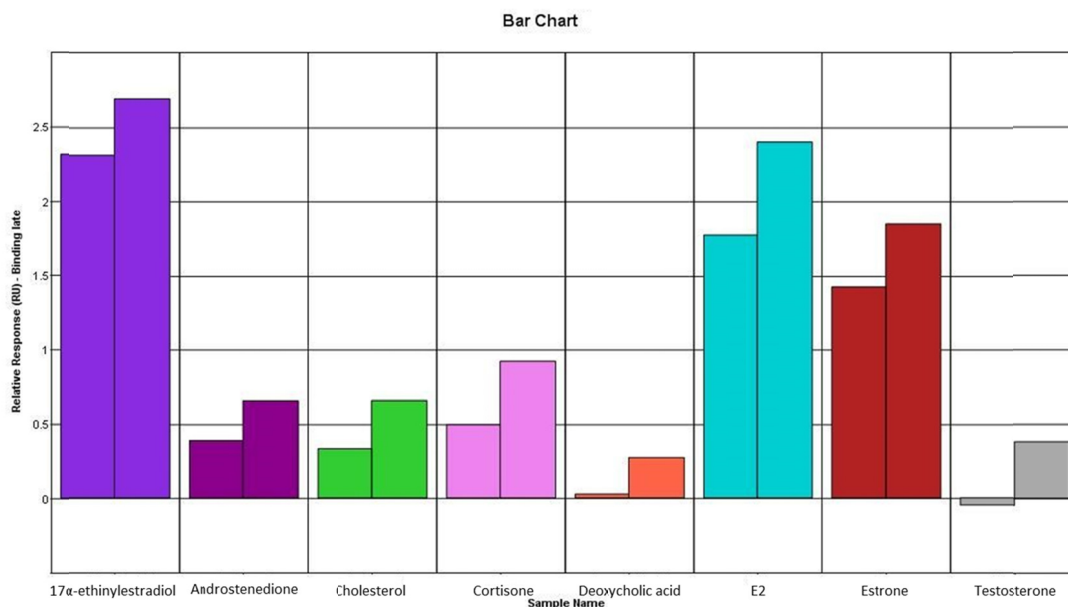


Figure 24: Solvent-corrected and blank-subtracted relative binding responses of E2 and structurally related cholesterol derivatives to sequence 1.

Combining the obtained results in SPR with the structural analysis of the different molecules confirms a structural similarity, especially in the phenolic group A (red circle), for  $17\alpha$ -ethinylestradiol, E2, and Estrone. A high affinity to chemicals with a phenolic group A indicates that this part of the molecule acts as the most important epitope (binding site) for the selected aptamers. This cross-reactivity of the aptamers was expected considering the structural difference between E2 as the target and Nortestosterone as the counter molecule during the SELEX. The differences in response values between binding and non-binding chemicals to sequence 1 and 2 can be ascribed to the number of double bonds in ring A, which has an effect on the molecular structure of ring A from flat with 3 double bonds (aromatic ring) in  $17\alpha$ -ethinylestradiol, E2 and Estrone, to boat- or chair-shape with no double bonds in Deoxycholic acid and Cholesterol. Testosterone, Androstenedione, and Cortisone with a ring A containing one double bond and a ketone group also showed a low binding response to sequence 1 and 2. Furthermore, the specificity of sequence 1 and 2 for  $17\alpha$ -ethinylestradiol, E2 and Estrone can also be explained by the existence of  $\text{CH}_3$  groups near ring A in Deoxycholic acid, Cholesterol, Testosterone, Androstenedione, and Cortisone, by the presence of a number of electron pushing atoms, such as oxygen, which can lead to a different charge distribution over the molecules, as well as by the size of the side chain attached to ring D (blue circle). Comparing the specificity of the selected aptamers in this project with the Kim *et al.* aptamer shows that, because of their epitope specificity, our sequence 1 and 2 are more advantageous and reliable than the Kim *et al.* aptamer with a unclear epitope specificity.



## 4. Conclusion

This thesis project sprung from the prototype E2 aptasensor introduced by Kim *et al.* (2007), and was aimed to develop a new SELEX process for the selection of E2-aptamers in an optimized buffer composed of PBS and 10% ethanol, while Nortestosterone was used as counter molecule. It was hypothesized that such a SELEX can select aptamers with a high affinity and specificity to E2, especially for its hydroxylated aromatic ring A (phenolic group), according to the structural difference between E2 and Nortestosterone. Moreover, it was assumed that optimization of the buffer conditions for SELEX will allow, on the one hand, adequate dissolving of E2, and on the other hand, the selection of aptamers in experimentally realistic conditions. It was expected that selected aptamers in such realistic conditions will show lower unspecific binding and cross-reaction to molecules that are structurally similar to E2. Therefore, a more specific aptamer would be selected to fabricate a more efficient E2 aptasensor.

As a first step, 12 iterative SELEX cycles were carried out on a pre-designed 80-mer ssDNA library, which was dissolved in the optimized buffer. After sequencing and structural analysis, the SELEX ended up with two aptamer molecules for E2.

In the next step, both chemically synthesized biotinylated aptamers were immobilized on an SA-modified SPR sensor chip for affinity and specificity analysis. Under experimentally realistic conditions (e.g. PBS with 10% ethanol buffer, at RT) both selected sequences 2 and 1 showed good KDs (0.947 vs. 7.666  $\mu\text{M}$ , respectively), as well as a broad range of detection (0.36-11.47  $\mu\text{M}$  and 1.44-22.95  $\mu\text{M}$ , respectively) for E2.

Specificity studies indicated a high selectivity of both sequence 2 and 1 for cholesterol derivatives with a phenolic group A epitope (17 $\alpha$ -ethinylestradiol, E2 and Estrone). In contrast to a previously selected 76-mer aptamer by Kim *et al.*, this epitope selectivity of the aptamers is due to a SELEX process targeting the structural difference between E2 and Nortestosterone. This advantageous characteristic of our selected aptamers can give a highly reliable detection in complex samples.

It is important to note that this is the first time that a prototype SPR-based aptasensor is fabricated for E2, while previous efforts by Kim *et al.* were unsuccessful. One of the most important challenges in this project was a low *Rmax* for both aptamers, due to the small molecular weight of E2. This low *Rmax* results in a low sensitivity of the system. To overcome this problem, further optimization of the system, such as immobilization level, flow rate, etc., is suggested. Also, application of innovative methodologies, such as strand displacement, can improve the situation. In this method, specific aptamers for the target molecule are hybridized with a complementary sequence that is attached on the sensor surface. Exposure to the target molecules results in the detachment of the aptamers from the complementary sequence while they are attaching to the target molecules. This indirect assay can result in an improved *Rmax* via displacement of the massive aptamer molecule instead of the binding of a small molecule.

Furthermore, during this project an E2 sandwich assay with a secondary aptamer for E2 was performed in an attempt to increase the sensitivity and decrease the detection limit. The secondary aptamer was previously selected at the biosensor group of Hasselt University. The secondary aptamer was selected during iterative SELEX cycles for E2, while Dexamethasone was used as the counter molecule. Based on structural differences of E2 and Dexamethasone, it was assumed that the secondary aptamer probably can bind to a different epitope of E2 in comparison with the immobilized aptamers 1 and 2 on the sensor chip. In this assay, it was hypothesized that a huge response can be

detected by sending E2 complexed with the secondary aptamer over the sensor. The obtained results did not follow the hypothesis, and indicated that the secondary aptamer probably trapped the E2 molecule completely, so the aptamer on the sensor surface could not bind to E2. Further experiments are suggested.

As the last point, it is important to state that optimization of such a new SELEX in this thesis will allow to select various highly specific aptamers, each directed against a different epitope of E2. These aptamers can be selected to develop an array system for the precise distinction between E2 and structurally similar molecules. Because of the ability of different E2 aptamers to each probe a specific part of the target molecule (epitope), an array of E2 aptamers is necessary for the accurate discrimination of E2 from other structurally similar molecules. Potentially, such a developed array system can be used by scientists and environmental care systems to reliably detect EDCs in complex environmental samples (e.g. waste water) as well as in biological samples. However, reaching these desirable goals requires solving problems such as selection of different aptamers that selectively recognize different epitopes of the target molecule, as well as testing their binding ability by changing the working conditions from experimental buffers to natural samples. When this is achieved, the array system can be patented and fabricated commercially.

However, this thesis project was a great step forward to fabricate an aptasensor, for real-time detection and measurement of E2 in an easier, faster, and cheaper way in comparison with other techniques, but stills more research and development is necessary.

## References

1. Monosik, R., Stredansky, M., Sturdik E. 2012. Biosensors – classification, characterization and new trends. *Acta Chimica Slovaca*. 5(1); pp. 109-120.
2. Jiang, J.Q., Yin, Q., Zhou, J.L., Pearce, P. 2005. Occurrence and treatment trials of endocrine disrupting chemicals (EDCs) in wastewaters. *Chemosphere*. 61; pp. 544–550.
3. Diamanti-Kandarakis, E., Bourguignon, J.P., Giudice, L.C., Hauser, R., Prins, G.S., Soto, A.M., Zoeller, R.T., Gore A.C. 2009. Endocrine-Disrupting Chemicals: An endocrine society scientific statement. *Endocrine Reviews*. 30(4); pp. 293–342.
4. Bergman, A., Heindel, J.J., Jobling, S., Kidd, K.A., Zoeller, R.T. 2013. *State of the science of endocrine disrupting chemicals - 2012*. Geneva: World Health Organization. ISBN: 9789241505031.
5. Kim, Y.S., Jung, H.S., Matsuura, T., Lee, H.Y., Kawai, T., Gu, M.B. 2007. Electrochemical detection of 17 $\beta$ -Estradiol using DNA aptamer immobilized gold electrode chip. *Biosensors and Bioelectronics*. 22; pp. 2525–2531.
6. Damstra, T., Barlow, S., Bergman, A., Kavlock, R., Van Der Kraak, G. 2002. *International Program on Chemical Safety: Global Assessment of the State-of-the-science of Endocrine Disruptors*. WHO /pcs /edc/02.2. Geneva: World Health Organization.
7. Unuvar, T., Buyukgebiz, A. 2012. Fetal and neonatal endocrine disruptors. *Journal of Clinical Research in Pediatric Endocrinology*. 4(2); pp.51- 60.
8. Lemke, T.L., Williams, D.A., Roche, V.F., Zito, S.W. 2012. *Foye's Principles of Medicinal Chemistry*. 7th ed. Philadelphia (PA): Lippincott Williams & Wilkin. ISBN: 9781609133450.
9. Kiparissis, Y., Balch, G.C., Metcalfe, T.L., Metcalfe, C.D. 2003. Effects of the isoflavones genistein and equol on the gonadal development of Japanese medaka *Oryzias latipes*. *Environmental Health Perspectives*. 111(9); pp. 1158-1163.
10. Kolpashchikov, D.M. 2012. An Elegant Biosensor Molecular Beacon Probe: Challenges and Recent Solutions. *Scientifica*. 2012; pp. 1-17.
11. Vermeeren, V., Wenmackers, S., Wagner, P., Michiels, L. 2009. DNA sensors with diamond as a promising alternative transducer material. *Sensors*. 9(7); pp. 5600-5636.
12. D'Orazio, P. 2011. Biosensors in clinical chemistry-2011 update. *Clinica Chimica Acta*. 412(19); pp. 1749-1761.
13. Sadana, A. 2003. *Biosensors: kinetics of binding and dissociation using fractals*. 1st ed. The Netherlands: Elsevier. ISBN: 9780444515124.
14. Mehrvar, M., Abdi, M. 2004. Recent developments, characteristics, and potential applications of electrochemical biosensors. *Analytical Sciences*. 20(8); pp. 1113-1126.

15. Thaler, M., Buhl, A., Welter, H., Schreiegg, A., Kehrel, M., Alber, B., Metzger, J., Lippa, P.B. 2009. Biosensor analyses of serum autoantibodies: application to antiphospholipid syndrome and systemic lupus erythematosus. *Analytical and bioanalytical chemistry*. 393(5); pp. 1417-1429.
16. Huang, L., Reekmans, G., Saerens, D., Friedt, J.M., Frederix, F., Francis, L., Muyldermans, S., Campitelli, A., Van Hoof, C. 2005. Prostate-specific antigen immunosensing based on mixed self-assembled monolayers, camel antibodies and colloidal gold enhanced sandwich assays. *Biosensors and Bioelectronics*. 21(3); pp. 483-490.
17. Chandra Bose Gopinath, S. 2007. Methods developed for SELEX. *Analytical and bioanalytical chemistry*. 387; pp. 171–182.
18. Tombelli, S., Minunni, M., Mascini, M. 2005. Analytical applications of aptamers. *Biosensors and Bioelectronics*. 20; pp. 2424–2434.
19. Sampson, T. 2003. Aptamers and SELEX: the technology. *World Patent Information*. 25; pp. 123–129.
20. Stoltenburg, R., Reinemann, C., Strehlitz, B. 2007. SELEX - A (r)evolutionary method to generate high-affinity nucleic acid ligands. *Biomolecular Engineering*. 24; pp. 381–403.
21. Wozei, E., Hermanowicz, S.W. 2006. Developing a yeast-based assay protocol to monitor total oestrogenic activity induced by 17 $\beta$ -oestradiol in activated sludge supernatants from batch experiments. *Water S.A.* 32; pp. 355-364.
22. Hahn, T., Tag, K., Riedel, K., Uhlig, S., Baronian, K., Gellissen, G., Kunze, G. 2006. A novel estrogen sensor based on recombinant *Arxula adenivorans* cells. *Biosensors and Bioelectronics*. 21; pp. 2078-2085.
23. Lin, X., Li, Y. 2006. A sensitive determination of estrogens with a Pt Nano-Clusters/Multi-Walled carbon nanotubes modified glassy carbon electrode. *Biosensors and Bioelectronics*. 22; pp. 253-259.
24. Wei, Y., Qiu, L., Yu, J.C.C., Lai, E.P.C. 2007. Molecularly imprinted solid phase extraction in a syringe needle packed with Polypyrrole-encapsulated carbon nanotubes for determination of Ochratoxin A in Red Wine. *Food Science and Technology International*. 13; pp. 375-380.
25. Vanbrabant, J., Vanschoenbeek, K., Vanoppen, E., Michiels, L. 2011. qPCR as a tool for enrichment analysis in the SELEX process. 2nd International Conference on Bio-Sensing Technology. 10-12 October. Amsterdam, The Netherlands.
26. Zuker, M. 2003. Mfold web server for nucleic acid folding and hybridization prediction. *Nucleic Acids Research*. 31 (13); pp. 3406-3415.
27. Kikin, O., D'Antonio, L., Bagga P.S. 2006. QGRS Mapper: a web-based server for predicting G-quadruplexes in nucleotide sequences. *Nucleic Acids Research*. 34(2); W676-W682.

28. Nagaraj, V.H., O'Flanagan, R.A., Sengupta, A.M. 2008. Better estimation of protein-DNA interaction parameters improve prediction of functional sites. *BMC Biotechnology*. 8(94); pp. 1-11.
29. Dorak, M.T. 2007. *Real-time PCR: BIOS advanced methods*. New York: Taylor & Francis. ISBN: 0203967313.
30. Chen, J., Sahota, A., Stambrook, P.J., Tischfield, J.A. 1991. Polymerase chain reaction amplification and sequence analysis of human mutant adenine phosphoribosyltransferase genes: the nature and frequency of errors caused by Taq DNA polymerase. *Mutation Research*. 249(1); pp. 169-176.
31. Amita, J., Vandana, T., Guleria, R.S., Verma, R.K. 2002. Qualitative evaluation of mycobacterial DNA extraction protocols for polymerase chain reaction. *Molecular Biology Today*. 3; pp. 43-50.
32. Karlsson, R. 1999. Affinity analysis of non-steady-state data obtained under mass transport limited conditions using BIAcore technology. *Journal of Molecular Recognition*. 12(5); pp. 285-292.
33. Karlsson, R. 2004. SPR for molecular interaction analysis: a review of emerging application areas. *Journal of Molecular Recognition*. 17(3); pp. 151-161.
34. Holmberg, A., Blomstergren, A., Nord, O., Lukacs, M., Lundeberg, J., Uhlén, M. 2004. The biotin-streptavidin interaction can be reversibly broken using water at elevated temperatures. *Electrophoresis*. 26(3); pp. 501-510.
35. Patching, S.G. 2013. Surface plasmon resonance spectroscopy for characterisation of membrane protein–ligand interactions and its potential for drug discovery. *Biochimica et Biophysica Acta*. 1838(2014); pp. 43–55.
36. Schasfoort, R.B.M., Tudos, A.J. 2008. *Handbook of Surface Plasmon Resonance*. Cambridge: RSC Publishing. ISBN: 9780854042678.
37. Cooper, M.A. 2004. Advances in membrane receptor screening and analysis. *Journal of Molecular Recognition*. 17; pp. 286-315.

## Auteursrechtelijke overeenkomst

Ik/wij verlenen het wereldwijde auteursrecht voor de ingediende eindverhandeling:

**Optimization of a new SELEX process for the selection of novel 17 $\beta$ -estradiol aptamers**

Richting: **master in de biomedische wetenschappen-bio-elektronica en nanotechnologie**

Jaar: **2014**

in alle mogelijke mediaformaten, - bestaande en in de toekomst te ontwikkelen - , aan de Universiteit Hasselt.

Niet tegenstaand deze toekenning van het auteursrecht aan de Universiteit Hasselt behoud ik als auteur het recht om de eindverhandeling, - in zijn geheel of gedeeltelijk -, vrij te reproduceren, (her)publiceren of distribueren zonder de toelating te moeten verkrijgen van de Universiteit Hasselt.

Ik bevestig dat de eindverhandeling mijn origineel werk is, en dat ik het recht heb om de rechten te verlenen die in deze overeenkomst worden beschreven. Ik verklaar tevens dat de eindverhandeling, naar mijn weten, het auteursrecht van anderen niet overtreedt.

Ik verklaar tevens dat ik voor het materiaal in de eindverhandeling dat beschermd wordt door het auteursrecht, de nodige toelatingen heb verkregen zodat ik deze ook aan de Universiteit Hasselt kan overdragen en dat dit duidelijk in de tekst en inhoud van de eindverhandeling werd genotificeerd.

Universiteit Hasselt zal mij als auteur(s) van de eindverhandeling identificeren en zal geen wijzigingen aanbrengen aan de eindverhandeling, uitgezonderd deze toegelaten door deze overeenkomst.

Voor akkoord,

**Khorshid, Mehran**

Datum: **17/01/2014**